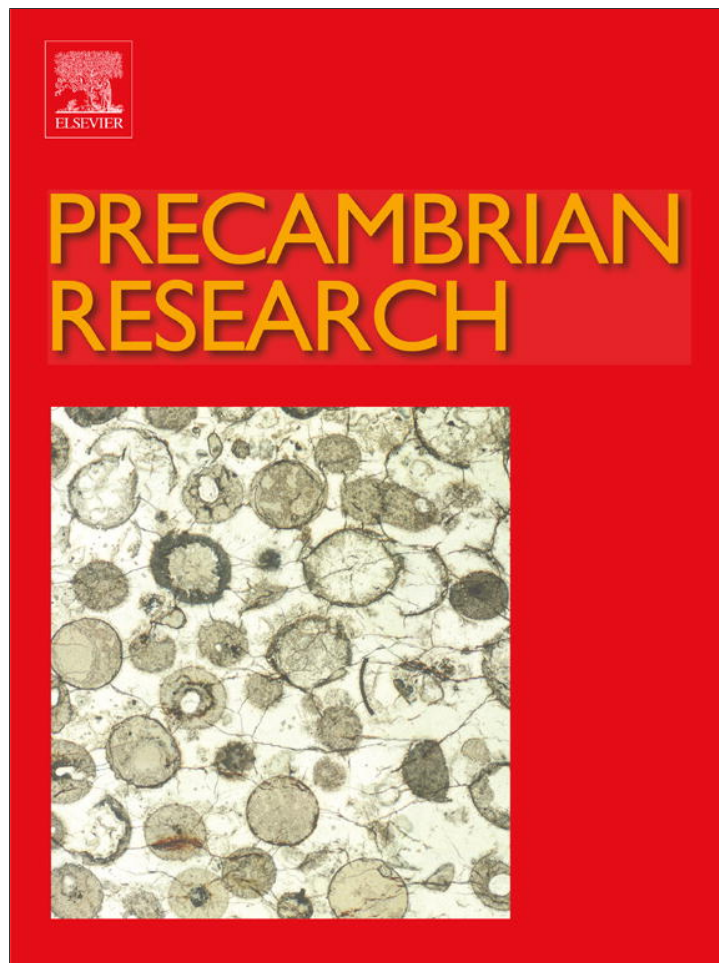


Provided for non-commercial research and education use.
Not for reproduction, distribution or commercial use.



(This is a sample cover image for this issue. The actual cover is not yet available at this time.)

This article appeared in a journal published by Elsevier. The attached copy is furnished to the author for internal non-commercial research and education use, including for instruction at the authors institution and sharing with colleagues.

Other uses, including reproduction and distribution, or selling or licensing copies, or posting to personal, institutional or third party websites are prohibited.

In most cases authors are permitted to post their version of the article (e.g. in Word or Tex form) to their personal website or institutional repository. Authors requiring further information regarding Elsevier's archiving and manuscript policies are encouraged to visit:

<http://www.elsevier.com/copyright>

Contents lists available at [SciVerse ScienceDirect](http://www.sciencedirect.com)

Precambrian Research

journal homepage: www.elsevier.com/locate/precamres

The Mesoproterozoic Karagwe–Ankole Belt (formerly the NE Kibara Belt): The result of prolonged extensional intracratonic basin development punctuated by two short-lived far-field compressional events

M. Fernandez-Alonso^{a,*}, H. Cutten^b, B. De Waele^c, L. Tack^a, A. Tahon^a, D. Baudet^a, S.D. Barritt^d

^a Department of Earth Sciences, Royal Museum for Central Africa, Tervuren, Belgium

^b Geological Survey of Western Australia, Department of Mines and Petroleum, East Perth, WA 6004, Western Australia, Australia

^c SRK Consulting, West Perth, WA 6005, Western Australia, Australia

^d GeoWitch Consulting, 1411 LK Naarden, The Netherlands

ARTICLE INFO

Article history:

Received 28 October 2011

Received in revised form 4 June 2012

Accepted 10 June 2012

Available online xxx

Keywords:

Karagwe–Ankole Belt

Akanyaru Supergroup

Kagera Supergroup

Provenance analysis

Mesoproterozoic basin evolution

Rodinia and Gondwana amalgamations

ABSTRACT

The Mesoproterozoic Kibara Belt (also Kibaran Belt or Kibarides in some references) of Central Africa was often portrayed as a continuous, c. 1500 km long orogenic belt, trending NE to NNE from Katanga, Democratic Republic of Congo (DRC) in the south, up into SW Uganda in the north. Recently however, the Karagwe–Ankole Belt (KAB; formerly the NE Kibara Belt) has been redefined as the part north of a NW oriented Palaeoproterozoic basement high of the Ubende–Rusizi Belts, while the Kibara Belt (KIB) is now limited to the part south of this rise.

We present a lithostratigraphy for the KAB that takes into account two rheologically contrasting structural domains (Western and Eastern Domain); each of them being characterised by independent sedimentary sub basin(s) and depositional conditions: the ED with Archaean basement versus the WD with Palaeoproterozoic basement. We document new volcanic and detrital U–Pb SHRIMP zircon data which provide new constraints on the timing of deposition and on the detrital provenance of the sedimentary sequences in the KAB. We discuss the evolution of the KAB in a wider regional context, comparing it to other Mesoproterozoic units and with reference to the general geodynamic history of this part of the African continent in Proterozoic times.

The lithostratigraphic successions of the KAB are only valid respectively in the ED (Kagera Supergroup) or in the WD (Akanyaru Supergroup), with no correlations between them. Deposition of the Kagera Supergroup in the ED is bracketed between 1.78 Ga and 1.37 Ga and the deposits have to be considered an Eburnean-age “molasse”. Detrital components comprise material only of Archaean and Palaeoproterozoic age, consistent with derivation from nearby source regions. In the WD, deposition of the two lowermost groups of the Akanyaru Supergroup is bracketed between 1.42 Ga and 1.37 Ga. The large contribution of detrital Palaeoproterozoic components in the WD strengthens the view that this domain is underlain by Palaeoproterozoic basement and supports the concept that part of the Akanyaru Supergroup sediments consists of reworked Eburnean-aged molasse. In the WD of the Kivu–Maniema area (DRC), later sedimentation periods are documented at respectively 1222 Ma and 710 Ma. The KAB documents a long-lived period of intracratonic intermittent depositional activity (with periods of interruption of deposition, erosion and magmatism) showing a recurrent subsidence trend controlled by structural activity moving with time from E to W.

On a regional scale, we postulate that since 1.8 Ga, following the amalgamation of Archaean and Palaeoproterozoic landmasses into a single coherent ‘proto-Congo Craton’, various long-lived shallow-water intracratonic basins (aulacogenes) developed. These basins underwent a comparable Mesoproterozoic geodynamic evolution, as shown not only in the sequences of the KAB and of the relatively close Kibara (KIB), Bangweulu Block and Northern Irumide Belts, but even in more distant sequences located in SW Angola and E Brazil.

The long-lived aulacogene history of the KAB within the proto-Congo Craton is interrupted only twice by short-lived compressional deformation reflecting far-field effects of global orogenic events, external to the proto-Congo Craton. The first event at 1.0 Ga is related to Rodinia amalgamation. The second event at 550 Ma results from Gondwana amalgamation and develops a N–S Pan African overprint in the KAB which has previously been underestimated or even overlooked. Three mineralisation provinces

* Corresponding author at: Leuvense Steenweg, 13, B-3080 Tervuren, Belgium. Tel.: +32 2 7695431.

E-mail address: max.fernandez@africamuseum.be (M. Fernandez-Alonso).

occurring in the KAB, respectively the Bushveld-type, the tin-coltan-wolfram and the gold province, can be ascribed successively to the 1375 Ma Kibaran magmatic event, the 1.0 Ga Rodinia and the 550 Ma Gondwana amalgamation events.

Our results give additional weight to the recent redefinition of the KAB and the KIB, forming two distinct Belts respectively north and south of the Palaeoproterozoic basement high of the Ubende-Rusizi Belts, the more that within this basement rise local Mesoproterozoic strike-slip basins, with their own unique lithostratigraphic and geodynamic characteristics (e.g. Itiaso Group) are documented, which differ from those of the KAB or the KIB.

© 2012 Elsevier B.V. All rights reserved.

1. Introduction

The Mesoproterozoic Kibara Belt (also Kibaran Belt or Kibarides in some references) of Central Africa is often portrayed as a continuous, c. 1500 km long orogenic belt, trending NE to NNE from Katanga, Democratic Republic of Congo (DRC) in the south, up into SW Uganda in the north (e.g. Brinckmann et al., 2001). Satellite imagery however, supports older schematic representations (e.g. Furon, 1958; Cahen and Snelling, 1966) showing that this belt consists of two distinct northern and southern segments (Fig. 1). These two are separated in the DRC between the Katanga and Kivu-Maniema regions by a NW-trending basement rise, partially consisting of a Karoo-age (Late Carboniferous to Early Jurassic) rift, itself superimposed on the Palaeoproterozoic Rusizi Belt (Lepersonne, 1974; Lavreau, 1985), which extends beneath Lake Tanganyika, and links up with the Palaeoproterozoic Ubende Belt of SW Tanzania (Klerkx et al., 1987; Theunissen et al., 1996). The apparent paradox of Palaeoproterozoic belts cross-cutting a Mesoproterozoic Kibara Belt results from repeated, to the present day, crustal-scale structural reactivation along the pre-existing Ubendian-Rusizian structures (Klerkx et al., 1998).

The two segments of the Belt, north and south of the basement rise, have been redefined by Tack et al. (2010) as (1) the Karagwe-Ankole Belt (KAB), spanning Rwanda and Burundi, SW Uganda and NW Tanzania as well as the Kivu-Maniema region of the DRC and (2) the Kibara Belt (KIB) further SW in the Katanga region, including the Kibara Mountains type area near Mitwaba town (Fig. 1).

Recent zircon U–Pb SHRIMP magmatic ages, laser ablation zircon Hf data and ^{40}Ar – ^{39}Ar dating have shown that the magmatism in the KAB results from a major intracratonic (c. 1375 Ma) bimodal event (Tack et al., 2010). This event consists of widespread, voluminous S-type granitoid rocks (Fernandez-Alonso et al., 1986) with accompanying subordinate mafic intrusive rocks and the 350 km-long mafic-ultramafic Kabanga–Musongati alignment (KM) of layered Bushveld-type complexes (Deblond, 1994; Tack et al., 1994; Deblond and Tack, 1999). The KM alignment is emplaced in a 10–35 km-wide arc-shaped boundary zone between two structurally contrasting domains in the KAB: a Western Domain (WD) and an Eastern Domain (ED) (Fig. 2).

Tack et al. (2010) have shown that the coeval magmatic suites originate in a regional-scale intracratonic setting under an extensional (transtensional) regime, and proposed to restrict the use of the term 'Kibaran event', only to this prominent extensional phase. This event pre-dates compressional deformation of the KAB. Later magmatic events occurred at c. 1205 Ma (A-type granitoids) and c. 986 Ma (tin-granites) (Tack et al., 2010). These represent minor additions to the crust, although the c. 986 Ma event forms the Central African Sn–Nb–Ta–W–Au metallogenic province (Pohl, 1994; Dewaele et al., 2007a,b, 2008a,b, 2010; De Clercq et al., 2008).

In this paper, we build on Tack et al. (2010), on the 1:250,000 scale geological map of the KAB (Fig. 3; Fernandez-Alonso, 2007) and on new detrital and volcanic zircon U–Pb SHRIMP data. We also discuss published and unpublished data, airborne geophysics and metasedimentary sequences of the KAB. We propose a consistent belt-wide lithostratigraphy, document timing of sedimentation

and evolution of the KAB sedimentary basins and propose an intracratonic evolution for the KAB within a wider regional setting.

2. General setting of the Karagwe-Ankole Belt

2.1. Two structurally contrasting domains

The Karagwe-Ankole Belt (KAB) is characterised by two structurally contrasting domains: the Western Domain (WD) and the Eastern Domain (ED) separated by a boundary zone, the Kabanga–Musongati (KM) alignment comprising mafic and ultramafic layered complexes (Fig. 2).

The WD consists of deformed, greenschist- to amphibolite facies metasedimentary rocks and subordinate inter-layered metavolcanic units intruded by numerous extensive massifs of S-type c. 1375 Ma granitoids which are devoid of economic minerals and by the c. 986 Ma tin-granites with accompanying mineralisation. In Rwanda, these rocks overly crystalline basement of Palaeoproterozoic age (Fernandez-Alonso and Theunissen, 1998; Tack et al., 2010). The WD corresponds to strongly deformed parts of the KAB. Contacts between the S-type granitoids and the parent metasedimentary rocks or crystalline basement are intrusive or tectonic.

The ED is characterised by an eastwards decrease of both deformation and metamorphism (Tack et al., 1994). A basal conglomerate in the ED unconformably overlies either gneissic basement, which is part of the Archaean Tanzania Craton, or the Palaeoproterozoic Ruwenzori Fold Belt. In contrast to the WD, the ED is devoid of S-type granitoids and economic mineralisation.

2.2. Airborne geophysical data

Most of the area occupied by the KAB has been covered by a number of local geophysical surveys including gravimetry, magnetometry and gamma-ray spectrometry, collected between 1974 and 1981. Although a continent-wide geophysical compilation was carried out in the early 1990s as part of the African Magnetic Mapping Project (AMMP – ITC, The Netherlands, and Leeds University, UK), most of this data remained proprietary and only subsets had been released for academic work (e.g. Nyakaana et al., 1999). In 2002, one of the co-authors (Barritt) reprocessed part of this data into a single georeferenced dataset of the KAB and surrounding regions at 200 m-resolution. This provided additional support for the model by Tack et al. (1994) of the two contrasting structural domains of the KAB, previously based only on field evidence.

Geophysically, the boundary zone including the KM alignment between the WD and ED is expressed as a magnetically textured arc (Figs. 2 and 4). The intrusions, in the field in Burundi and Tanzania, including a hidden body at depth (underneath the Nkoma Group in Burundi) are revealed by a strong anomaly apparent in the Total Magnetic Intensity image (TMI) (Fig. 4). In Burundi there is agreement between the field observation and aeromagnetic data (Fig. 5a). However, in Tanzania the arc coincides with a 5–10 km-wide band of subdued quartzite ridges with intercalated pelites, which become dominantly pelitic in the south in the area to the

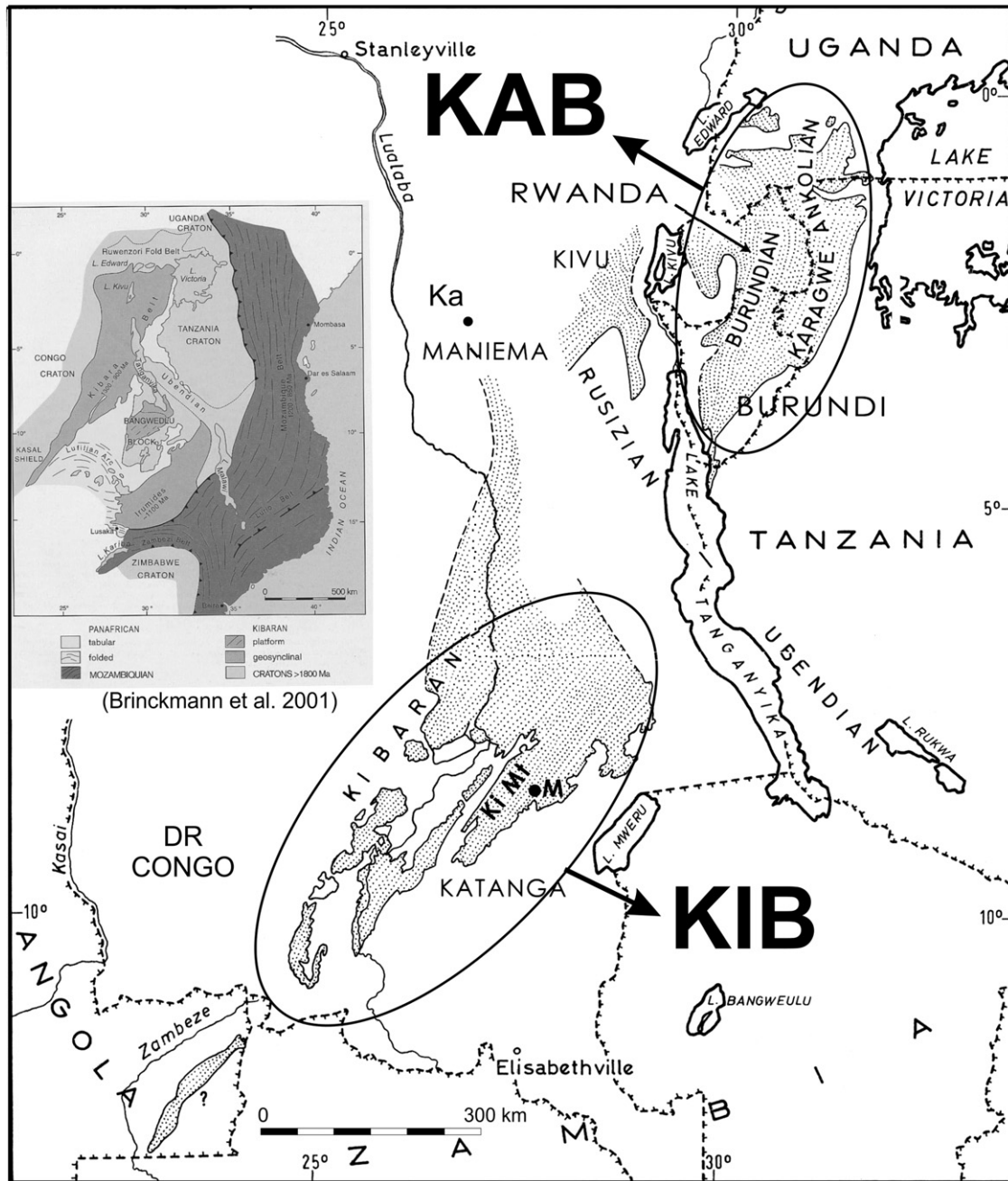


Fig. 1. Sketch map (Cahen and Snelling, 1966), showing the Karagwe-Ankole Belt (KAB) and the Kibara Belt (KIB) as redefined by Tack et al. (2010). Inset after Brinckmann et al., 2001 showing the Kibara Belt as one single and continuous belt. Ki Mt, Kibara Mountains type locality; M, Mitwaba town; Ka, Kalima town.

west of the Nyakahura (Tanzania)-Mugera (Burundi) inlier of the Archaean Tanzania Craton. Here, the KM layered complexes visible in the aeromagnetic survey images are shifted to the east, compared to the field observations of Tack et al. (1994) (Fig. 5b). Moreover, both aeromagnetic data and gravimetry data show that the western palaeogeographic limit of the Archaean Craton (western limit of ED) is marked by an indenter tip, whose prominent role during compressional events in the KAB will be outlined further in this paper.

2.3. The northern limit of the KAB

In SW Uganda, where published systematic field mapping dates back to the early 1960s, the location of the northern limit between the WD and the Palaeoproterozoic Ruwenzori Fold Belt (Fig. 1, inset) remains poorly constrained. Recent geochemical and isotopic

work by Buchwaldt et al. (2008) supports however in general, the location of the limit proposed by Fernandez-Alonso (2007). Based on zircon geochronology and Sm-Nd isotopic investigation of four granitoid massifs, Buchwaldt et al. (2008) recognise two distinct terranes (separated by the dashed line A-B, Fig. 3): (1) a northern terrane characterised by c. 1565 Ma and c. 1445 Ma granitic magmatism, and (2) a southern terrane characterised by S-type granite magmatism dated c. 1367–1330 Ma.

The data of the northern terrane are consistent with two analyses of the Muramba granite (Tack et al., 2010) with dates of 1460 Ma and 1525 Ma, suggesting these represent inherited material of Palaeoproterozoic origin. They agree also with preliminary unpublished isotopic data on the Masha granitoid (Fig. 3, M) located in the northern terrane and which yielded a Rb-Sr age of 1637 ± 89 Ma and a bulk zircon age of 1947 ± 6 Ma (Liégeois,

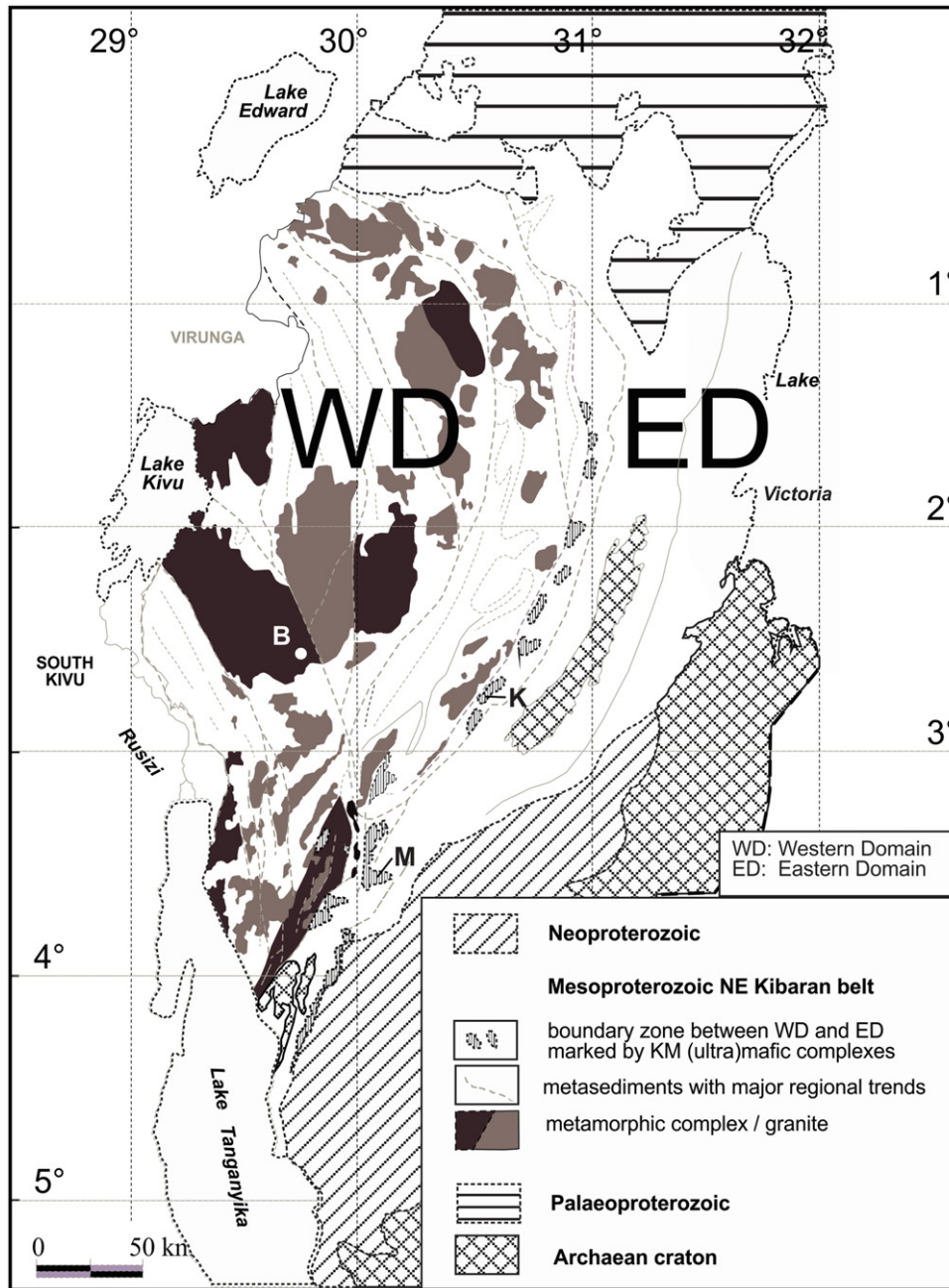


Fig. 2. Regional framework of the Karagwe-Ankole Belt (KAB) (after Tack et al., 1994; Fernandez-Alonso, 2007). K, Kabanga massif (Tanzania); M, Musongati massif (Burundi); B, Butare town (Rwanda).

pers. comm.). We suggest that these early Mesoproterozoic to late Palaeoproterozoic ages reflect the nearby occurrence of the Ruwenzori fold Belt in SW Uganda.

The ages given by Buchwaldt et al. (2008) for the southern terrane, characterised by S-type granite magmatism, are in agreement with those of Tack et al. (2010) for the KAB.

Locating more precisely the boundary between the KAB and the Ruwenzori Fold Belt will hopefully be resolved by new aeromagnetic data recently collected in Uganda.

3. New uniform belt-wide lithostratigraphy of the KAB

3.1. Earlier lithostratigraphic concepts

In general, the metasedimentary rocks of the KAB consist mainly of siliciclastic shallow-water deposits (pelite and arenite

successions). Lateral and vertical facies changes are frequent and may be extreme, varying from starved basins to proximal turbiditic environments, shallow siliciclastic flats and/or deltaic zones. Carbonate rocks are scarce and restricted to lenticular deposits. There is also evidence of some felsic explosive volcanic activity, including vitroclastic tuffs and breccias.

Attempts to constrain the lithostratigraphy of the Mesoproterozoic units had been undertaken separately in Rwanda, Burundi, D. R. Congo Kivu-Maniema, NW Tanzania and SW Uganda over a 50-year period (see Cahen and Lepersonne, 1967; Cahen et al., 1984 for an exhaustive overview) resulting in confusing stratigraphic terminologies for the different (sub)regions.

Little attention has previously been paid to understanding the depositional environment of the sedimentary successions. A general lack of distinctive marker horizons, as well as the presence of overprinting contact metamorphism, folding and faulting, and the

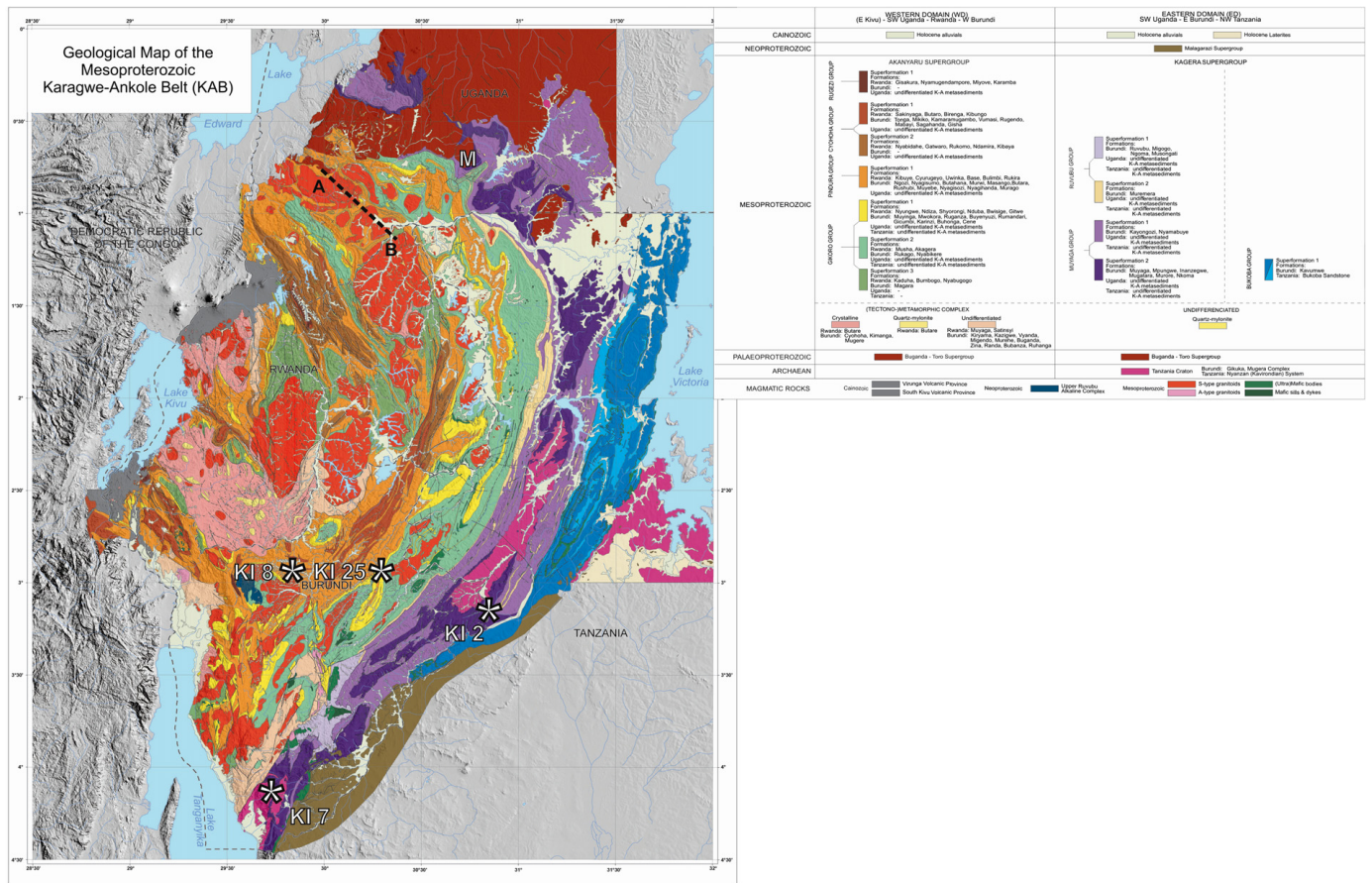


Fig. 3. Simplified geological map and legend of the Mesoproterozoic Karagwe-Ankole Belt (KAB) (from Fernandez-Alonso, 2007). Black dashed line (A-B): assumed terrane boundary according to Buchwaldt et al. (2008); M, Masha granitoid (Uganda); KI 2, KI 7, KI 8 and KI 25, location of 4 dated samples.

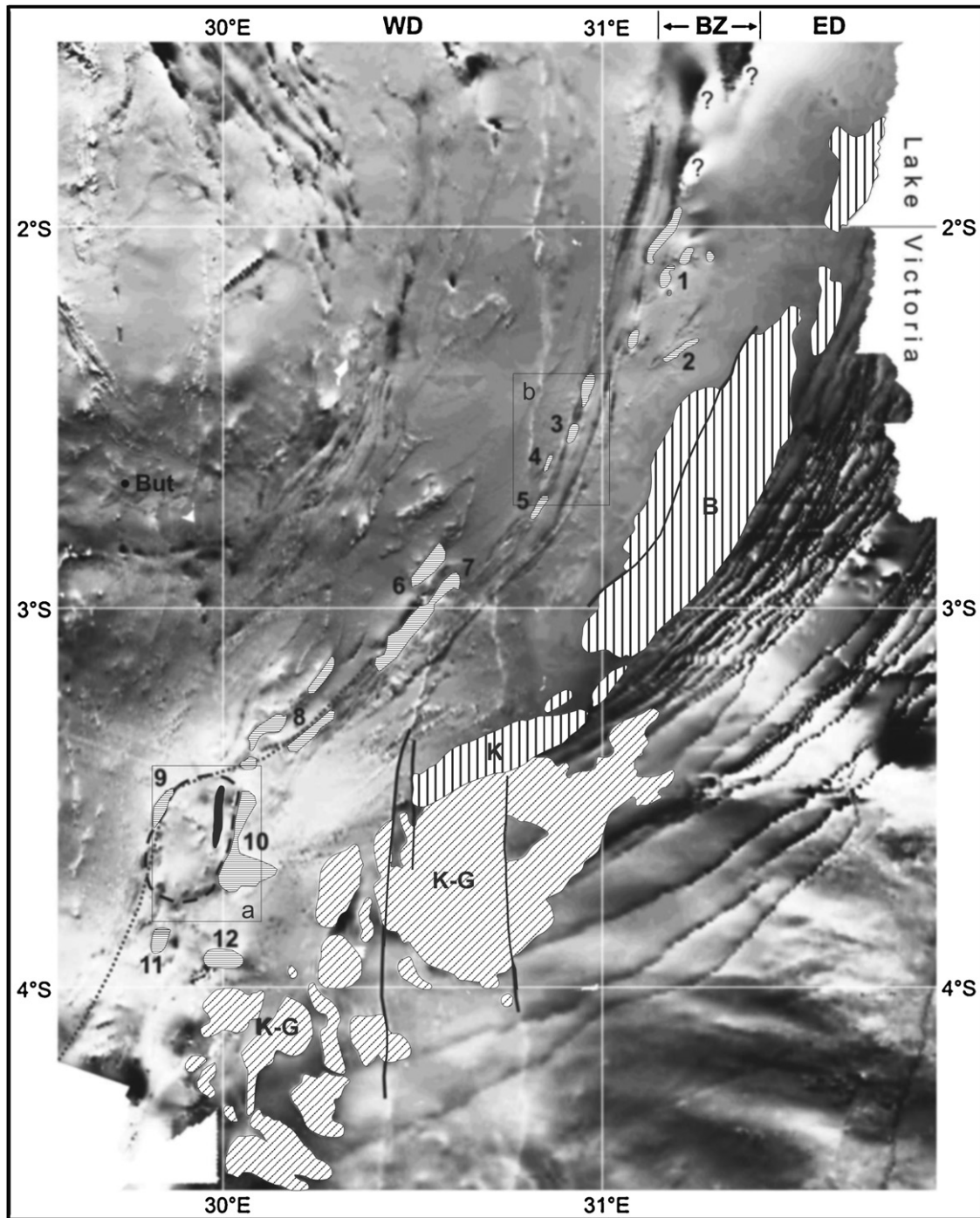


Fig. 4. Regional interpretation of the contrast-enhanced Total Magnetic Intensity (TMI) map over the E part of the Karagwe-Ankole Belt (KAB). *top line*: WD: Western Domain; BZ, boundary zone, ED, Eastern Domain. *numbers*: mafic/ultramafic layered complexes of the KM-alignment – 1: Burigi – 2: Ruiza – 3: Kibamba – 4: Kanyautenge – 5: Luhuma – 6: Kabanga – 7: Mulemera – 8: Nyabikere – 9: Waga – 10: Mukanda-Buhoro-Musongati – 11: Rutovu – 12: Nkoma (not outcropping); ?, potential new bodies at depth; *But*, Butare town (Rwanda). *B, K*, region occupied by 1375 Ma gabbro-noritic sills intrusive in tabular siliciclastic rocks of the Bukoba Group of the ED; *B*, Bukoba Sandstone formation, *K*, Kavumwe formation. *K-G*, region covered by 795 Ma Neoproterozoic Kabuye-Gagwe amygdaloidal Continental Flood Basalts. *Dashed line*: outline of elliptical gravimetric structure (Burundi) and region of N-S elongated bodies of 1205 Ma A-type granitoid rocks. *Dotted line*: contact between WD and ED, highlighting the western palaeogeographic limit of the Archaean Tanzania craton, marked by an indenter tip located near the Waga massif (9); note that the gravimetric structure coincides with the indenter tip. *Solid lines*: Faults. *Box*: location of Fig. 5a and b.

fact that the successions of the KAB span several countries, severely limited correlation attempts across the region.

A first stratigraphic correlation attempt throughout the whole region was given by Cahen et al. (1984) who referred to (1) a Kibaran Supergroup in Shaba (Katanga) (based on Cahen and Snelling, 1966; Cahen and Lepersonne, 1967); (2) a Burundian Supergroup in NE Rwanda (based on Gérards and Lepersonne, 1964); (3) a Burundian

Supergroup in E Burundi (based on Waleffe, 1966); and (4) a Karagwe-Ankolean Supergroup in Tanzania (based on Gray, 1967).

3.1.1. Burundi

Waleffe (1966) formalised a threefold subdivision for the pelite and arenite successions in Burundi into the Burundian Group with Lower, Middle and Upper Burundian units. The base of the

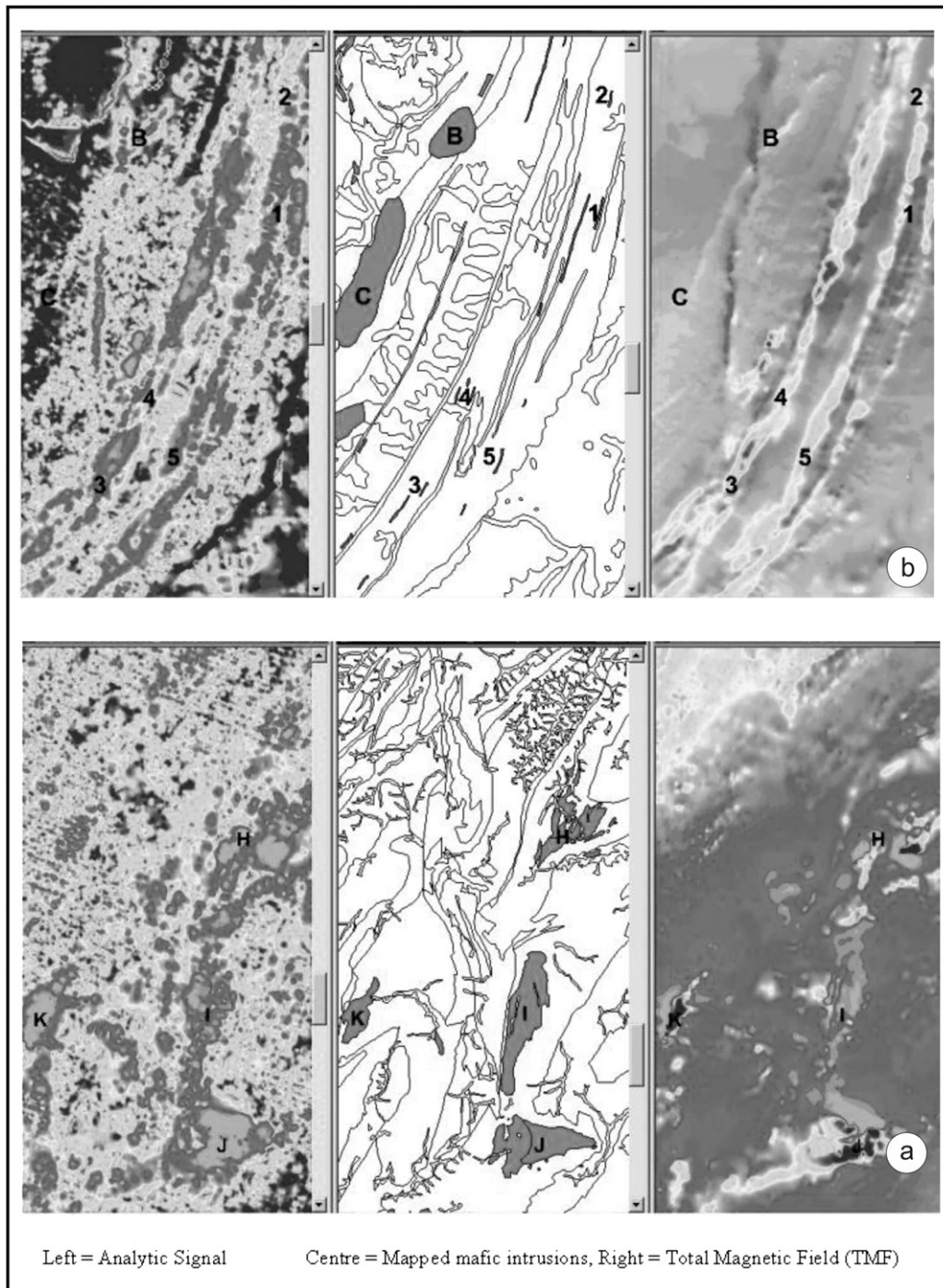


Fig. 5. Analytical signal, field evidence and total magnetic intensity of KM layered complexes in Burundi and Tanzania. (a) Aeromagnetics and field data are in agreement: H, Nyabikere massif; K, Waga massif; I, Mukanda-Buhoro massif; J, Musongati massif. (b) Aeromagnetic data show shift to the east relative to the field mapping data; 1–5: aeromagnetic bodies; B and C: two (unnamed) bodies from field data in Tack et al. (1994) with no geophysical signal.

Lower Burundian can be observed in eastern Burundi resting unconformably upon the Nyakahura-Mugera inlier of the Archaean Tanzania Craton (locally the Mugera granite). The successions generally dip towards the NW. Despite the recognition of extensive folding and thrust-duplication, *Waleffe (1966)* overestimated the thicknesses of the Lower, Middle and Upper Burundian to be 11,500 m, 2500 m and more than 1350 m, respectively. The metasediments of the Muyaga unit (in the ED) as well as of the northern Nkoma region display various evidence of felsic explosive

volcanic activity, including vitroclastic tuffs and breccias (see Section 4.1, sample KI 2) (*Navez and Karayenga, 1990; Tack et al., 1992*).

Regional correlation attempts for the entire country have never been published, nor has an overall formal stratigraphic column for the entire Burundian Group. The general 1:250,000 scale geological map of Burundi (*Anonymous, 1990*) gives only a generalised stratigraphic column, which comprises a series of unnamed units, existing at specific stratigraphic and/or structural positions.

3.1.2. Tanzania and Uganda

In Tanzania, the Karagwe-Ankolean Supergroup consists of pelitic and psammitic metasedimentary rocks, unconformably overlying the Nyakahura-Mugera inlier of the Archaean Tanzania Craton. Calcareous beds are absent, and coarse clastic sediments (conglomerates and arkoses) predominate at the base (Van Straaten, 1984). These indicate palaeo-current directions from E to W, from the Archaean Craton into the developing KAB basin. Most of the successions however consist of quartzites and phyllites. On the 1:2,000,000 scale *Geology and Mineral map of Tanzania* (2008), the lithostratigraphic terminology refers to Mesoproterozoic Karagwe-Ankolean detrital sediments with a ≥ 1.37 Ga time constraint after Tack et al. (2002a,b, 2010).

In Uganda, the Karagwe-Ankolean Supergroup is also characterised by argillaceous units intercalated with thinner bands of quartzites and quartzitic sandstones. The northern boundary of the Karagwe-Ankolean is poorly constrained (see Section 2.3) but the supergroup is considered to overlie the Palaeoproterozoic Buganda-Toro Supergroup of the Ruwenzori fold Belt (Cahen et al., 1984; Master et al., 2008). The unconformity is apparent in the Mashonga sedimentary outlier of Uganda (Pohl and Hadoto, 1990). Contacts with the Archaean Tanzania Craton have not been observed.

3.1.3. Rwanda

In the 1950s it was recognised (Cahen, 1952; Peeters, 1956) that the central and eastern part of Rwanda showed a similar deformation pattern as in Burundi. In contrast, the western part of Rwanda is structurally more complex. This contrast has hampered correlation with the rest of the country and with Burundi (Gérards and Lepersonne, 1964).

Field mapping and sedimentological analysis in the late 1980s have delineated distinct shear-bounded tectonostratigraphic domains (Tahon, 1990; Fernandez-Alonso and Theunissen, 1998) each with unique lithostratigraphic successions (Baudet et al., 1988). Some correlations from domain to domain were possible, considering lateral facies variations. Baudet et al. (1988) and Theunissen et al. (1991) established a formal Rwanda Supergroup lithostratigraphy comprising four successive groups of predominantly siliciclastic composition with a total thickness of between 2500 m and 5000 m; respectively from bottom to top: the Gikoro, Pindura, Cyohoha and Rugezi Groups.

The c. 1375 Ma S-type granitoid intrusions are restricted to the lowermost Gikoro and Pindura Groups and do not extend into the overlying Cyohoha and Rugezi Groups. The base of the supergroup could not be defined as it is always either in fault contact with a tectono-metamorphic complex of inferred older age, or in intrusive contact with S-type granitoids (Baudet et al., 1988). Field and geochronological evidence indicate that part of the tectono-metamorphic Butare complex (SW Rwanda) belongs to the Palaeoproterozoic basement (Gérards and Ledent, 1970; Fernandez-Alonso and Theunissen, 1998; Tack et al., 2010).

The depositional environment of the Rwanda Supergroup indicates a shallow-water basin (or sub basins) with depocentres ranging from proximal turbiditic via coastal (lagunar, intertidal mudshelves) to fluvial (fanglomerates, deltaic) environments (Baudet et al., 1988). Sedimentary structures suggest that transport in the different depocentres was from N to S in the northern part of Rwanda, E to W in the eastern part and SW to NE in the south western part (Baudet, personal communication). Abrupt facies changes and erosional surfaces indicate tectonic controls. In the Pindura Group, bimodal volcanic intercalations are present, best described in W Burundi (Ntungicimpaye, 1981, 1983, 1984; Ntungicimpaye and Tack, 1992; Tack and Ntungicimpaye, 1993; Ntungicimpaye and Kampunzu, 1987; Brinckmann et al., 2001) but also documented in SW Rwanda (Pohl, 1987; Baudet et al., 1988; Jung and

Meyer, 1990). Dark shales and carbonate lenses were deposited only after felsic volcanism had been emplaced.

3.1.4. The Nkoma–Kavumwe (Burundi) and Bukoba Sandstone (Tanzania) units

The stratigraphic position of the Nkoma and Kavumwe units in Burundi (Cahen et al., 1984) and Bukoba Sandstone in Tanzania (Cahen et al., 1984), which have been attributed as part of the Neoproterozoic Malagarazi Supergroup of Burundi and equivalent Bukoban System of Tanzania (Tack, 1995) have been the subject of long debate. Field evidence in Burundi (Tack et al., 1992), geochemistry, palaeomagnetism, mineral potential (Tack, 1995) and $^{40}\text{Ar}/^{39}\text{Ar}$ geochronology of mafic intrusives (Deblond et al., 2001) indicate that the Nkoma unit and the Kavumwe-Bukoba Sandstone are Mesoproterozoic in age, and therefore have to be considered to be part of the KAB.

3.1.5. The Kivu-Maniema region, D. R. Congo

A structural continuity from W Rwanda and NW Burundi into the Kivu-Maniema region, north of the Ubende-Rusizi basement extension and west of the Western Rift can be seen in satellite imagery and from regional compilations (Figs. 1, 3 and 6). Hence, lithostratigraphy for Rwanda and Burundi should extend into this region and correlate with existing local stratigraphy. However, due to the extremely difficult field access, scarcity of data and its structural complexity, the Kivu-Maniema geology was loosely defined in older works while post-1960 field observations and laboratory constraints remain limited.

In the last four decades, independent and different local Burundian stratigraphies have been published for the most accessible part (c. 1000 km²) around Bukavu town (Fig. 6, insets 1 and 2) (Villeneuve and Guyonnet-Benaize, 2006; Rumvegeri et al., 2004; Walemba and Master, 2005).

Villeneuve (1980) suggested a two-fold subdivision with a major disconformity separating an upper Nya-Ngezie from a lower Bugarama unit. Detrital zircons dated at 1222 ± 28 Ma are documented from the base of the Nya-Ngezie unit (Villeneuve and Chorowicz, 2004) (Fig. 6).

3.2. Definition of a new uniform lithostratigraphy for the KAB: the Kagera Supergroup in the ED and the Akanyaru Supergroup in the WD

Since Cahen et al. (1984), further attempts to compile a Belt-wide stratigraphy of the KAB remained unsuccessful until the concept of two contrasting structural domains (WD and ED) introduced by Tack et al. (1994, 2010). Using this new concept as a working hypothesis, Fernandez-Alonso (2007) compiled, from published maps and unpublished documents, a new GIS-based geological map at the scale 1:250,000 (Fig. 3) and established a regional lithostratigraphy for the metasedimentary successions of the entire KAB, using the best available and constrained local (litho)stratigraphical information (Fig. 7).

Lithostratigraphic correlation between the WD and the ED domains is not possible as each is confined to independent sedimentary sub-basins.

In the ED (in E Burundi, NW Tanzania and SW Uganda), the Kagera Supergroup extends from well-documented E Burundi along-strike into NW Tanzania and SW Uganda (Fig. 3). (The name Kagera Supergroup comes from the administrative district in Tanzania covering most of this area, and is also the name of the river –also sometimes spelled as Akagera–marking the border between Tanzania and Rwanda.)

The Kagera Supergroup is found in two adjacent sub basins (Fig. 7), separated by a fault that may reflect some palaeogeographic setting. Each has its own lithostratigraphic column: (1) The western

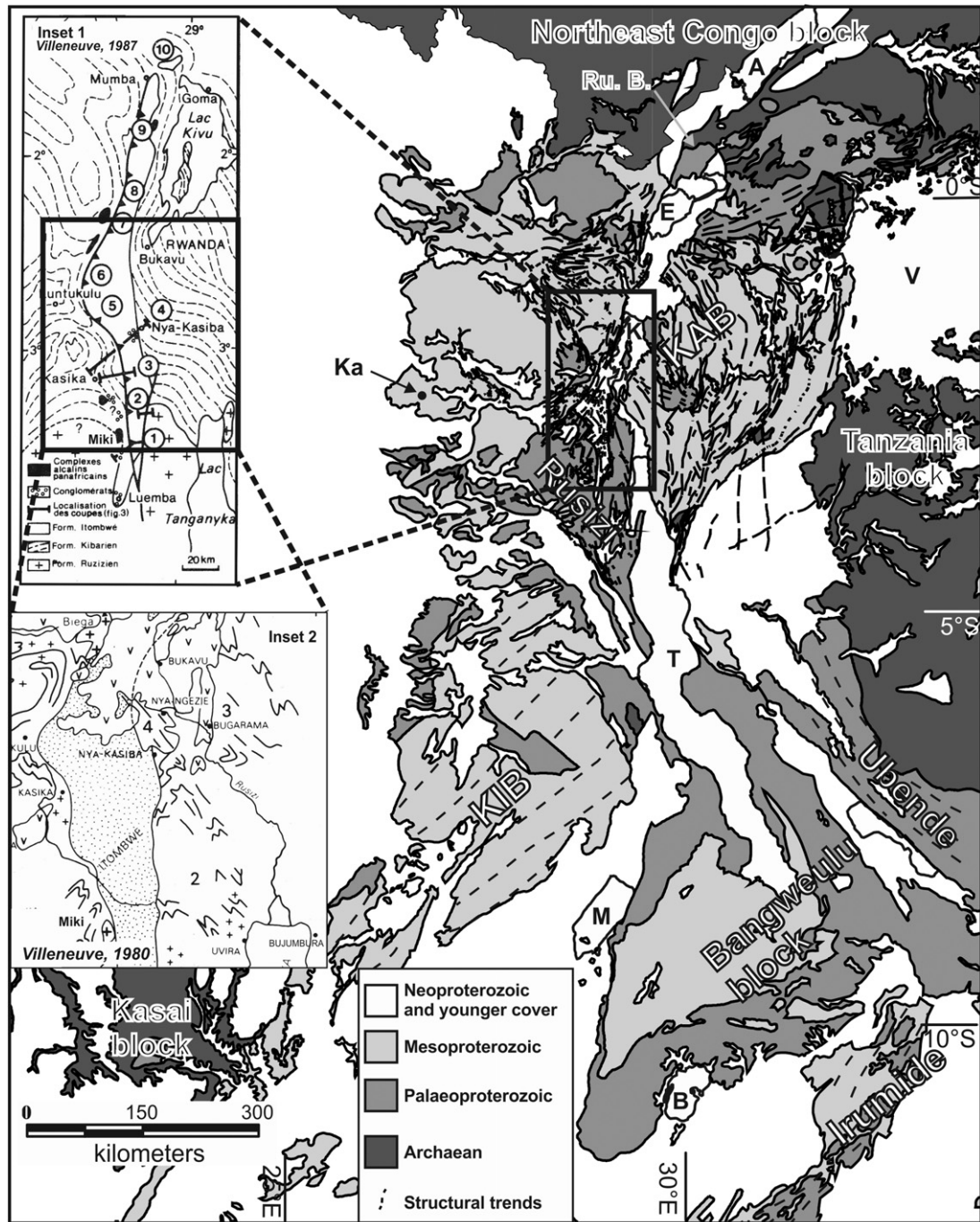


Fig. 6. Regional setting of the Karagwe-Ankole Belt (KAB) in its Proterozoic and Archaean framework (in Fernandez-Alonso, 2007 after CGMW, 1986–1990). Lakes are named after their initial: A, Albert; E, Edward; V, Victoria; K, Kivu; T, Tanganyika; M, Mweru and B, Bangweulu. Ru. b., Eburnean-aged Ruwenzori Fold Belt; Ka – Kalima town. Note the NW–SE trending Ubende – Rusizi basement high highlighting lack of continuity between the Karagwe – Ankole Belt (KAB) and the Kibara Belt (KIB). Inset 1 (after Villeneuve, 1987): sketch map of the narrow and N–S elongated Itombwe “Syncline” in the Kivu region of the DRC. Inset 2: sketch map of central part of the Itombwe “Syncline” (after Villeneuve, 1980). Kasika: location of 986 Ma Sn-granite, Nya-Kasiba: location of the basal unconformity, Nya-Ngezies and Bugarama: local type areas.

sub basin, contains the Muyaga and overlying Ruvubu Groups, i.e. the former Lower Burundian Group (Waleffe, 1966; Anonymous, 1990) and former Neoproterozoic Nkoma unit (see Section 3.1.4) (Waleffe, 1966; Tack et al., 1992; Tack, 1995) and (2) the eastern sub basin contains the former Neoproterozoic Bukoba Group (see Section 3.1.4), i.e. the Bukoba Sandstone and Kavumwe units of Waleffe (1966) and Tack (1995).

In the WD (in Rwanda, W Burundi and SW Uganda), the Rwanda Supergroup lithostratigraphy defined by Baudet et al. (1988) and Theunissen et al. (1991) was used to correlate along-strike to the

north and south with less documented lithostratigraphic columns in W Burundi and SW Uganda (Fig. 3). This redefines the Rwanda Supergroup as the Akanyaru Supergroup (the Akanyaru river forms part of the boundary between Rwanda and Burundi), which includes respectively (from bottom to top), the Gikoro, Pindura, Cyohoha and Rugezi Groups (Fig. 7). Although no unconformity has been recognised, geological mapping in Rwanda and Burundi suggests a stratigraphic (and depositional) break between the lower Gikoro–Pindura and the upper Cyohoha–Rugezi units (Baudet et al., pers. comm.). The fact that the 1375 Ma S-type granitoid rocks

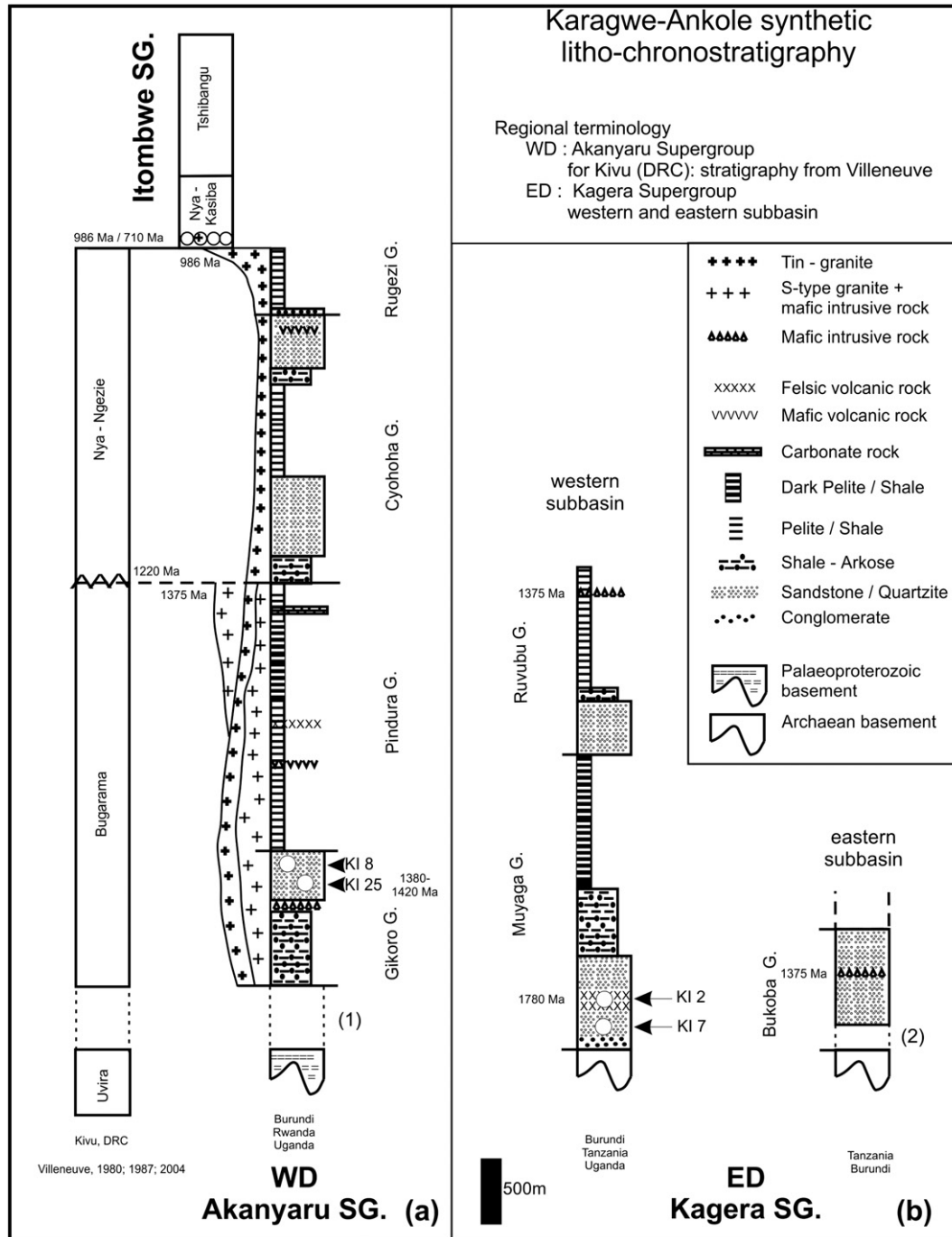


Fig. 7. Synthetic litho-chronostratigraphic logs of the KAB for the WD (a) and ED (b) with position of 4 dated samples (KI 2, KI 7, KI 8 and KI 25, this work) and available magmatic and detrital zircon age constraints (this work and literature). (1) Contact between Palaeoproterozoic basement and Gikoro Group is tectonic or intrusive; (2) unconformable contact of Bukoba Group on Archaean basement not observed.

intrude only the Gikoro and Pindura Groups, but never the overlying Cyohoha and Rugezi Groups, further strengthens the possibility of a stratigraphic break.

Theunissen (1988, 1989) and Klerkx et al. (1987) ascribed the well-developed pervasive S₁-fabric (typically sub parallel to bedding surfaces S₀) in the lower Gikoro-Pindura metasedimentary units to have developed during extensional emplacement of the S-type granitoid rocks. This S₁ fabric weakens upwards and is not present in the Cyohoha-Rugezi Groups. The total sedimentary pile (or Gikoro-Pindura only?) at the time of intrusion of the S-type granitoid rocks may have been ±15 km in thickness before partial removal and denudation, as estimated from the depth of intrusion

at 2–5 Kbar for the S-type granitoids (Fernandez-Alonso et al., 1986).

4. New depositional ages and provenance analysis for the KAB

New single-zircon U–Pb SHRIMP age determinations were obtained from four locations within Burundi: two in the ED, one volcanoclastic rock (magmatic zircons) and one quartzite (detrital zircons), and two in the WD, from quartzites (Figs. 3 and 7). Details of these analyses are listed in Table 1. All mean ages are quoted in the text with 95% confidence intervals, and analytical procedures

Table 1

Ion microprobe single-zircon U–Pb SHRIMP data of analysed magmatic and detrital zircons: KI 2 (Murore Tuff)=RG 145.838; KI 7 (Nyanza-Lac Quartzite)=RG 161.714; KI 8 (Ruganza Quartzite)=RG 142.387; KI 25 (Muyinga Quartzite)=RG 84.332. RG code refers to sample identifier in the RMCA – Tervuren (Belgium) reference collections.

Spot	f_{206} %	U (ppm)	Th (ppm)	Th/U	$^{238}\text{U}/^{206}\text{Pb}$ $\pm 1\sigma$	$^{207}\text{Pb}/^{206}\text{Pb}$ $\pm 1\sigma$	$^{207}\text{Pb}/^{206}\text{Pb}$ age $\pm 1\sigma$ (Ma)	%C	
KI2-1	0.040	360.6	435.5	1.25	3.13549	± 0.06763	1799.1	± 11.2	99.2
KI2-2	0.262	216.8	149.4	0.71	2.97749	± 0.06530	1886.9	± 14.3	98.9
KI2-3	0.090	325.0	221.7	0.70	3.16598	± 0.06833	1772.5	± 10.9	99.8
KI2-4	0.149	279.0	142.4	0.53	3.17565	± 0.06841	1770.0	± 11.3	99.7
KI2-5	0.243	229.7	162.2	0.73	3.17116	± 0.06856	1758.0	± 15.9	100.5
KI2-6	0.061	195.4	136.4	0.72	3.11648	± 0.06901	1796.4	± 12.7	99.9
KI2-7	0.077	198.4	134.9	0.70	3.14019	± 0.06843	1781.6	± 12.6	100.0
KI7-1	0.104	85.8	84.7	1.02	2.96946	± 0.06742	1906.9	± 21.7	98.1
KI7-2	0.072	286.1	235.9	0.85	2.72387	± 0.06036	2017.3	± 9.7	99.9
KI7-3	2.340	261.2	443.3	1.75	3.13015	± 0.06965	1879.4	± 71.5	95.1
KI7-4	–	298.7	68.3	0.24	1.94152	± 0.04197	2596.8	± 6.9	103.1
KI7-5	0.014	85.8	146.1	1.76	2.79435	± 0.06374	1969.9	± 16.0	100.1
KI7-6	–	52.8	58.3	1.14	2.99776	± 0.07162	1934.4	± 21.8	95.9
KI7-7	0.606	35.7	26.6	0.77	2.03130	± 0.05124	2559.7	± 24.6	100.8
KI7-8	0.230	1948.8	1111.0	0.59	2.84272	± 0.05964	1846.2	± 5.2	105.2
KI7-9	1.250	220.0	233.2	1.10	2.09833	± 0.04526	2584.2	± 12.0	97.2
KI7-10	0.090	143.7	345.2	2.48	2.79606	± 0.06162	2019.9	± 14.1	97.6
KI7-11	0.529	208.2	234.8	1.17	2.74228	± 0.05932	1985.0	± 14.7	101.0
KI7-12	0.001	474.8	715.9	1.56	2.90789	± 0.06206	1889.6	± 12.4	100.8
KI7-13	6.009	222.7	105.9	0.49	2.77984	± 0.06085	2073.6	± 50.2	95.5
KI7-14	1.300	276.9	249.5	0.93	2.05128	± 0.04442	2636.1	± 17.3	97.1
KI7-16	1.197	231.4	444.2	1.98	2.09282	± 0.04530	2566.1	± 16.1	98.1
KI7-17	0.100	320.1	209.5	0.68	2.10474	± 0.04533	2559.7	± 7.3	97.9
KI7-18	1.022	260.8	290.4	1.15	2.15603	± 0.04690	2593.0	± 22.2	94.7
KI7-19	0.138	126.0	82.8	0.68	2.13762	± 0.04708	2419.3	± 11.8	102.3
KI7-20	0.047	116.5	73.3	0.65	2.44576	± 0.05412	2213.0	± 15.1	99.9
KI7-21r	2.128	175.6	211.8	1.25	2.24710	± 0.04886	2466.2	± 17.2	96.2
KI7-22	0.036	286.7	213.1	0.77	2.16916	± 0.04637	2401.8	± 7.2	101.8
KI7-21c	0.208	114.0	48.0	0.44	1.99683	± 0.04402	2586.0	± 12.1	101.2
KI7-23	1.792	31.1	44.3	1.47	2.10476	± 0.05266	2675.0	± 85.0	93.7
KI7-24	0.060	596.6	60.2	0.10	2.70543	± 0.05722	1980.9	± 7.0	102.4
KI7-25	0.465	118.7	149.6	1.30	2.98400	± 0.06616	1863.0	± 21.0	100.0
KI7-26	18.216	399.1	1350.2	3.50	2.28550	± 0.18652	1993.7	± 1195.0	117.4
KI7-27c	3.437	263.6	391.8	1.54	2.30277	± 0.04944	2470.7	± 18.4	94.1
KI7-28	0.052	132.8	46.7	0.36	1.96519	± 0.04312	2587.6	± 11.0	102.5
KI7-29	5.655	321.5	407.3	1.31	2.90372	± 0.06312	2003.8	± 71.2	95.2
KI7-30	1.550	182.7	216.1	1.22	2.08422	± 0.04519	2508.5	± 17.8	100.7
KI7-31	2.284	54.2	96.7	1.85	3.01406	± 0.07165	1969.6	± 52.3	93.8
KI7-32	0.053	187.3	101.3	0.56	2.03934	± 0.04409	2519.8	± 8.6	102.1
KI7-33	0.113	236.8	152.5	0.67	2.85409	± 0.06139	1976.8	± 11.3	98.0
KI7-34	0.141	129.6	142.2	1.13	2.94508	± 0.06490	1877.0	± 17.5	100.4
KI7-35	0.123	187.5	137.6	0.76	1.96733	± 0.04254	2594.7	± 8.4	102.1
KI7-36	0.686	907.6	342.3	0.39	3.66857	± 0.07862	2463.1	± 5.6	63.1
KI7-37	0.238	225.7	123.7	0.57	2.21370	± 0.04794	2491.1	± 6.8	96.5
KI7-38	0.182	85.1	64.7	0.79	2.10725	± 0.04685	2622.6	± 11.4	95.5
KI7-39	0.638	184.7	108.9	0.61	2.11093	± 0.04585	2588.0	± 8.3	96.6
KI8-1	0.390	205.0	225.1	1.13	2.20312	± 0.04783	2613.9	± 7.6	92.3
KI8-2	0.174	88.0	94.0	1.10	2.00890	± 0.04470	2572.5	± 10.2	101.2
KI8-3	0.075	212.1	84.5	0.41	2.09422	± 0.04571	2613.7	± 6.1	96.3
KI8-4	0.041	202.8	140.3	0.71	2.04447	± 0.04459	2560.5	± 7.5	100.2
KI8-5	0.115	130.4	124.7	0.99	1.97656	± 0.04332	2631.6	± 7.4	100.3
KI8-6	0.018	314.7	490.9	1.61	2.11029	± 0.04568	2563.6	± 4.6	97.5
KI8-7c	2.198	1463.6	4555.8	3.22	8.45302	± 0.18527	2168.2	± 7.1	33.2
KI8-7r	0.533	908.5	591.2	0.67	3.95553	± 0.08475	2028.8	± 8.4	71.6
KI8-8	0.054	337.8	212.4	0.65	2.25214	± 0.04853	2586.9	± 4.8	91.6
KI8-9	0.020	255.6	251.5	1.02	2.00910	± 0.04341	2650.1	± 5.1	98.3
KI8-10	0.094	172.9	227.0	1.36	2.35498	± 0.05135	2560.3	± 7.7	89.1
KI8-11	0.535	126.2	226.5	1.85	3.79304	± 0.08456	2043.8	± 17.6	73.8
KI8-12	0.022	387.0	287.8	0.77	2.01318	± 0.04328	2626.5	± 4.3	99.0
KI8-13r	0.038	379.7	55.9	0.15	1.92573	± 0.04141	2732.3	± 3.9	98.7
KI8-14	0.019	215.0	198.4	0.95	1.99805	± 0.04357	2627.2	± 5.5	99.6
KI8-15	0.740	37.5	21.7	0.60	1.93685	± 0.04537	2608.9	± 19.5	102.9
KI8-16	0.431	67.4	174.8	2.68	2.07034	± 0.05096	2705.1	± 12.9	93.9
KI8-17	0.330	162.4	56.0	0.36	2.14735	± 0.04682	2479.4	± 8.9	99.4
KI8-18	0.046	351.6	198.7	0.58	2.09062	± 0.04497	2606.4	± 4.2	96.7
KI8-19	0.091	244.3	312.8	1.32	2.12228	± 0.04588	2561.9	± 5.5	97.1
KI8-20	0.041	200.8	158.3	0.81	2.08221	± 0.04518	2562.3	± 6	98.7
KI8-21	0.117	72.2	23.8	0.34	2.07468	± 0.04644	2607.7	± 10.1	97.2
KI8-22	0.764	99.3	119.5	1.24	2.78745	± 0.06221	2013.9	± 22.9	98.1
KI8-23	0.252	799.7	653.1	0.84	3.64438	± 0.07827	2517.4	± 4.7	62.1
KI8-24	0.091	242.2	351.1	1.50	2.76692	± 0.05988	2052.2	± 7.9	96.9
KI8-25	0.067	314.8	128.9	0.42	2.37115	± 0.05109	2354.2	± 5.5	96.4
KI8-26	0.133	179.4	174.5	1.01	2.23128	± 0.04848	2547.5	± 6.7	93.7
KI8-27	0.154	153.0	40.2	0.27	2.52139	± 0.05500	2137.3	± 11.1	100.8

Table 1 (Continued)

Spot	f_{206} %	U (ppm)	Th (ppm)	Th/U	$^{238}\text{U}/^{206}\text{Pb}$	$\pm 1\sigma$	$^{207}\text{Pb}/^{206}\text{Pb}$	$\pm 1\sigma$	$^{207}\text{Pb}/^{206}\text{Pb}$ age	$\pm 1\sigma$ (Ma)	%C
KI8-28	0.108	202.9	154.4	0.79	2.19886	± 0.04773	0.17064	± 0.00069	2564.0	± 6.7	94.2
KI8-29	0.053	336.6	225.0	0.69	2.05703	± 0.04441	0.17877	± 0.00057	2641.5	± 5.3	96.7
KI8-30	0.156	358.0	591.1	1.71	3.23444	± 0.06969	0.16836	± 0.00059	2541.4	± 5.9	68.3
KI8-31	0.079	189.5	128.2	0.70	2.65521	± 0.05767	0.17433	± 0.00069	2599.7	± 6.6	79.3
KI8-32	0.089	294.8	234.1	0.82	2.06493	± 0.04453	0.17986	± 0.00057	2651.6	± 5.3	96.0
KI8-33	0.048	321.5	217.8	0.70	2.13032	± 0.04605	0.17073	± 0.0005	2564.8	± 4.9	96.7
KI8-34	0.111	327.7	228.2	0.72	2.48885	± 0.05364	0.16963	± 0.00054	2554.0	± 5.3	85.3
KI8-35	0.287	555.8	637.9	1.19	2.57624	± 0.05526	0.16711	± 0.00048	2528.9	± 4.8	83.6
KI8-36	0.089	245.4	151.5	0.64	2.21165	± 0.04778	0.17525	± 0.00057	2608.4	± 5.4	92.2
KI8-37	0.085	213.9	167.1	0.81	2.32560	± 0.05046	0.16988	± 0.00068	2556.5	± 6.7	90.2
KI8-38	0.156	70.3	34.1	0.50	2.16238	± 0.04857	0.18378	± 0.00128	2687.3	± 11.5	91.2
KI8-39	0.070	478.6	200.4	0.43	2.35829	± 0.05057	0.16897	± 0.00039	2547.5	± 3.9	89.5
KI8-40	0.069	216.3	179.3	0.86	2.46507	± 0.05342	0.13526	± 0.00057	2167.4	± 7.3	101.3
KI8-41	0.028	344.1	386.1	1.16	2.05933	± 0.04431	0.17562	± 0.00045	2611.9	± 4.3	97.7
KI8-42	0.126	190.8	87.4	0.47	2.18864	± 0.04751	0.17256	± 0.00067	2582.7	± 6.4	93.9
KI8-43	0.112	457.1	675.6	1.53	3.19855	± 0.06897	0.12776	± 0.00045	2067.4	± 6.2	84.8
KI8-44	0.085	219.0	227.1	1.07	2.07219	± 0.04485	0.17107	± 0.00060	2568.1	± 5.9	98.8
KI8-45	0.035	470.1	437.5	0.96	2.16620	± 0.04660	0.16998	± 0.00039	2557.4	± 3.8	95.7
KI8-46	0.119	494.2	422.3	0.88	2.36499	± 0.05073	0.16837	± 0.00041	2541.5	± 4.1	89.4
KI8-49	0.047	246.6	122.9	0.51	2.18039	± 0.04716	0.17285	± 0.00059	2585.5	± 5.7	94.1
KI8-50	0.164	190.7	136.0	0.74	2.30254	± 0.05001	0.17720	± 0.00072	2626.8	± 6.8	88.5
KI8-47	0.133	300.0	507.2	1.75	2.47146	± 0.05331	0.17488	± 0.00057	2604.9	± 5.4	84.1
KI8-48	0.099	290.6	123.1	0.44	2.07216	± 0.04469	0.17498	± 0.00082	2605.9	± 7.8	97.4
KI8-51	0.153	126.0	48.4	0.40	2.06374	± 0.04533	0.17288	± 0.00094	2585.7	± 9.0	98.5
KI25-1	0.100	133.1	118.4	0.92	2.87114	0.04339	0.11386	0.00084	1861.9	13.4	103.5
KI25-2	4.739	310.9	330.0	1.10	6.71977	0.10522	0.10988	0.00599	1797.4	99.2	49.8
KI25-3	0.119	257.2	198.2	0.80	2.88351	0.04128	0.12039	0.00065	1962.0	9.7	97.8
KI25-4	0.097	125.2	107.5	0.89	2.86727	0.04387	0.11522	0.00100	1883.4	15.7	102.4
KI25-5	1.634	197.2	433.3	2.27	4.43212	0.06594	0.11310	0.00330	1849.8	52.8	70.9
KI25-6	0.124	75.5	67.8	0.93	3.90886	0.06508	0.08981	0.00175	1421.4	37.3	103.3
KI25-7	2.378	1077.6	923.0	0.89	5.29569	0.07338	0.08787	0.00262	1379.6	57.3	80.8
KI25-8	0.324	91.7	92.3	1.04	2.57662	0.04084	0.12552	0.00133	2036.2	18.7	103.8
KI25-9	0.104	327.9	90.1	0.28	2.98982	0.04224	0.11272	0.00055	1843.7	8.9	100.9
KI25-10	0.034	337.9	568.4	1.74	2.89265	0.04085	0.11599	0.00053	1893.3	8.2	101.0
KI25-11	1.368	536.6	595.7	1.15	3.81363	0.05308	0.11814	0.00126	1928.2	19.1	77.9
KI25-12c	3.630	726.9	1336.8	1.90	4.93364	0.06840	0.11223	0.00141	1835.9	22.7	64.8
KI25-12r	0.353	396.2	176.4	0.46	3.05645	0.04285	0.11377	0.00071	1860.4	11.3	98.1
KI25-13	4.906	1045.6	1189.5	1.18	5.85138	0.08022	0.11087	0.00140	1813.7	23.0	56.1
KI25-14	0.324	85.4	88.4	1.07	2.86814	0.04656	0.11383	0.00146	1861.5	23.2	103.6
KI25-15	0.218	126.2	107.9	0.88	2.94788	0.04480	0.11347	0.00109	1855.7	17.4	101.5
KI25-16	0.139	102.3	55.8	0.56	2.53734	0.03963	0.12653	0.00119	2050.3	16.7	104.5
KI25-17	0.635	246.5	304.6	1.28	3.19180	0.04584	0.12393	0.00099	2013.5	14.2	87.3
KI25-18	0.603	406.2	642.1	1.63	3.36953	0.04719	0.11554	0.00075	1888.4	11.7	88.7
KI25-19	0.135	128.5	128.0	1.03	2.46091	0.04096	0.13335	0.00092	2142.5	12.0	102.6
KI25-20	2.247	1154.3	372.1	0.33	5.28443	0.07277	0.09600	0.00179	1547.8	35.1	72.2
KI25-21	0.282	84.6	51.0	0.62	1.89367	0.02998	0.17596	0.00129	2615.2	12.2	104.5
KI25-22	1.133	157.6	383.4	2.51	2.09191	0.03144	0.18182	0.00171	2669.6	15.6	94.3
KI25-23	1.312	298.7	1383.3	4.78	6.40092	0.09394	0.11996	0.00149	1955.7	22.1	47.8
KI25-24	0.113	145.9	75.4	0.53	1.96041	0.02923	0.17647	0.00093	2620.0	8.8	101.4
KI25-25	6.816	574.3	614.1	1.10	1.66618	0.42765	0.10079	0.02318	1638.7	426.9	184.9
KI25-26	4.358	509.9	1224.0	2.48	5.23909	0.07455	0.10917	0.00254	1785.5	42.4	63.1
KI25-27	0.074	267.1	103.3	0.40	1.91351	0.02723	0.18680	0.00080	2714.2	7.0	99.9
KI25-28	0.946	478.9	695.9	1.50	4.48107	0.06343	0.10654	0.00115	1741.0	19.8	74.6
KI25-29	0.125	71.2	29.0	0.42	1.81205	0.02941	0.19189	0.00138	2758.4	11.8	102.7
KI25-30	0.042	775.6	440.6	0.59	2.25536	0.03080	0.18163	0.00039	2667.8	3.5	88.7
KI25-31	0.571	99.2	95.1	0.99	2.93545	0.04618	0.11261	0.00153	1841.9	24.6	102.6
KI25-32	0.344	142.5	84.4	0.61	3.20847	0.04831	0.11873	0.00128	1937.2	19.3	90.3
KI25-33	0.320	95.9	68.2	0.74	2.93829	0.04661	0.11444	0.00133	1871.1	20.9	100.9
KI25-34	0.158	168.2	195.2	1.20	2.91740	0.04336	0.11178	0.00083	1828.6	13.5	103.9
KI25-35	0.391	120.7	124.4	1.07	2.11718	0.03255	0.16174	0.00119	2473.9	12.4	100.8
KI25-36	0.376	764.4	725.4	0.98	3.89702	0.05335	0.10563	0.00060	1725.3	10.4	85.3
KI25-37	0.358	572.3	182.6	0.33	2.10643	0.02930	0.18570	0.00053	2704.5	4.7	92.6
KI25-38	-0.118	119.7	102.9	0.89	1.94420	0.02957	0.18019	0.00119	2654.6	10.9	100.8
KI25-39	0.202	156.9	98.9	0.65	4.14964	0.06201	0.08934	0.00097	1411.5	20.9	98.6
KI25-40	0.149	46.8	18.4	0.41	1.76076	0.03086	0.19380	0.00164	2774.7	13.9	104.5
KI25-41	1.293	30.7	41.8	1.41	2.97566	0.06011	0.10684	0.00344	1746.2	59.0	107.0
KI25-42	0.115	179.1	190.1	1.10	2.90521	0.04251	0.11571	0.00090	1891.0	14.0	100.8
KI25-43	0.758	271.8	138.4	0.53	2.18977	0.03187	0.17200	0.00130	2577.2	12.6	94.1
KI25-44	0.525	530.9	496.2	0.97	2.74411	0.03834	0.18496	0.00092	2697.8	8.2	74.2
KI25-45	0.126	284.8	293.0	1.06	2.99268	0.04265	0.11306	0.00065	1849.1	10.3	100.5
KI25-46	0.220	326.4	261.7	0.83	2.90975	0.04129	0.11490	0.00067	1878.4	10.5	101.4
KI25-47	4.166	544.6	318.5	0.60	3.27675	0.04802	0.14943	0.00273	2339.4	31.2	73.4
KI25-48	0.278	104.6	105.4	1.04	2.87775	0.04448	0.11426	0.00130	1868.2	20.5	102.9
KI25-49	0.068	250.7	208.0	0.86	2.77756	0.04037	0.12817	0.00065	2073.0	9.0	95.6
KI25-50	1.285	235.8	238.1	1.04	3.82492	0.06053	0.10936	0.00554	1788.8	92.2	83.7
KI25-51	0.211	254.9	269.7	1.09	2.02759	0.02950	0.19225	0.00075	2761.5	6.4	93.6

Table 1 (Continued)

Spot	f_{206} %	U (ppm)	Th (ppm)	Th/U	$^{238}\text{U}/^{206}\text{Pb}$	$\pm 1\sigma$	$^{207}\text{Pb}/^{206}\text{Pb}$	$\pm 1\sigma$	$^{207}\text{Pb}/^{206}\text{Pb}$ age	$\pm 1\sigma$ (Ma)	%C
KI25-52	0.126	174.1	209.0	1.24	2.96127	0.04359	0.11515	0.00083	1882.3	13.0	99.6
KI25-53	0.062	215.6	108.0	0.52	1.84281	0.02703	0.19605	0.00074	2793.6	6.2	100.0
KI25-54	2.173	549.5	618.4	1.16	4.50062	0.06238	0.16315	0.00184	2488.6	19.0	52.0
KI25-55	3.405	481.7	1309.1	2.81	4.94686	0.08228	0.11208	0.00281	1833.4	45.4	64.7
KI25-56	1.114	878.5	622.1	0.73	2.82187	0.03857	0.18114	0.00065	2663.3	6.0	73.4
KI25-57	0.118	214.2	111.2	0.54	2.68159	0.03889	0.12718	0.00076	2059.3	10.5	99.2
KI25-58	1.016	356.8	138.6	0.40	2.93682	0.04216	0.12108	0.00188	1972.2	27.7	95.8
KI25-59	3.109	579.1	605.8	1.08	3.90292	0.07390	0.11068	0.01436	1810.6	235.8	81.2
KI25-60	0.547	311.9	211.3	0.70	3.10712	0.04389	0.11807	0.00081	1927.2	12.2	93.3
KI25-61	0.019	699.6	129.6	0.19	2.24939	0.03084	0.15537	0.00038	2405.8	4.1	98.6
KI25-62	2.399	478.7	585.9	1.26	3.36497	0.05959	0.11302	0.01428	1848.6	228.5	90.7
KI25-63	0.270	132.2	91.7	0.72	2.96914	0.04492	0.11455	0.00110	1872.9	17.4	99.9
KI25-64	0.073	319.2	106.5	0.34	1.86031	0.02617	0.18528	0.00057	2700.7	5.0	102.7

f_{206} = the proportion of common ^{206}Pb in the total ^{206}Pb ; Th/U = $^{232}\text{Th}/^{238}\text{U}$; %C = % concordance. All ratios and ages corrected for common Pb using measured ^{204}Pb and composition appropriate to the age of the zircon (Stacey and Kramers, 1975). KI2 analyses conducted during a single session. 16 CZ3 standard analyses yielded a 2σ error of the mean of 1.15%. KI7 analyses conducted during two separate sessions. Session 1: 16 CZ3 standard analyses yielded a 2σ error of the mean of 1.15%; Session 2: 14 CZ3 standard analyses yielded a 2σ error of the mean of 1.25%. KI8 analyses conducted during a single session. 14 CZ3 standard analyses yielded a 2σ error of the mean of 1.25%. KI25 analyses conducted during a single session. 13 CZ3 standard analyses yielded a 2σ error of the mean of 0.85%.

are detailed in Appendix A. The four samples are stored in the RMCA, Tervuren (Belgium) reference collection, identified by collection numbers (RG, Table 1) with accompanying field information.

4.1. Eastern Domain (ED)

Sample KI 2 (Figs. 3 and 7) was collected from a felsic tuff interlayered within the arenites of the Murore Formation (Muyaga Group–Kagera Supergroup) which form the base of the little deformed siliciclastic succession, unconformably overlying the Archaean Tanzania Craton. Seven zircons were analysed, each no larger than 150 μm , generally euhedral. Cathode-luminescence (CL) imaging of these showed well defined concentric zoning suggesting a primary igneous origin. Proportions of common Pb (i.e. the percentage of ^{206}Pb that is of non-radiogenic origin, of the total ^{206}Pb , is indicated by f_{206}) are very low, ranging from 0.04 to 0.26%. A concordant cluster of 6 zircons yielded a concordia age of 1780 ± 9 Ma interpreted as the crystallisation age of this felsic tuff (Fig. 8a). One older concordant zircon, with a $^{207}\text{Pb}/^{206}\text{Pb}$ age of 1887 ± 14 Ma is interpreted as a xenocryst (Table 1). The crystallisation age of the tuff constrains the depositional age of the base of the Kagera Supergroup. Previous dating attempts of the same rocks using Rb–Sr yielded an age of 1350 Ma (Klerkx et al., 1984, 1987).

Sample KI 7 (Figs. 3 and 7) was collected from a coarse-grained to conglomeratic part of the Murore Quartzite, part of the same Murore Formation as KI 2 but located along strike some 50 km further south. Thirty nine zircons were analysed and range in shape from poorly rounded to well-rounded and up to 200 μm in size. CL-imaging showed well developed concentric zoning patterns as well as a wide range of CL-response from very low to very high. f_{206} values are generally below 1% but range as high as 2.34%; Th/U ratios between 0.50 and 1.50 suggest these zircons are of magmatic origin. Thirty two of the total 39 zircons are over 90% concordant, and show two main age groupings, 2.67–2.40 Ga (51%) and 2.02–1.85 Ga (41%) (Fig. 8b and e). One concordant zircon yielded a $^{207}\text{Pb}/^{206}\text{Pb}$ age of 2213 ± 15 Ma outside the two main age groups. The older zircons are moderately to well-rounded and show well-developed concentric zoning patterns. The degree of roundness and length to width ratios from 3:1 to 2:1 suggest these zircons are derived from not too distant magmatic sources for this age grouping, and the variable CL-response suggests a number of different sources. The younger age cluster comprises subhedral to euhedral zircons which are generally only half the size of the older zircons. A variable CL-response similar to that observed in the older zircons suggest these also were derived from a variety of source rocks, which are likely magmatic as suggested by their Th/U ratios between 0.5 and

1.5. The youngest concordant zircon places the maximum deposition age of the Murore Quartzite at 1846 ± 5 Ma, in agreement with the 1780 Ma crystallisation age of the felsic tuff in the Murore Formation (Fig. 7).

4.2. Western Domain (WD)

Samples from two quartzite units with similar lithostratigraphic positions were collected near the base of the Gikoro Group in the WD (lowermost group of Akanyaru Supergroup).

Sample KI 8 (Figs. 3 and 7) was collected from the Ruganza Quartzite–Ruganza Formation. Twenty eight concordant analyses of detrital zircons were obtained from a total of 52 zircons with Th/U ratios ranging from 0.27 to 3.22. The dominant age group ranges 2.73–2.48 Ga (87%) with a smaller group at 2.07–2.01 Ga (10%). Additional analyses yielded ages of 2.35, 2.17 and 2.14 Ga (Fig. 8c and e). Zircons of the older age group range in size from 80 to 120 μm with length to width ratios of 2:1 to 1:1. These are subrounded to angular and some are subhedral and euhedral, and generally show well developed concentric zoning consistent with a magmatic origin. Variable CL response suggests a range of magmatic source lithologies. Zircons from the younger age group range in size from 90 to 100 μm and length to width ratio is generally 1:1. CL response is high to variable and zircons display broad concentric zoning patterns. The youngest detrital zircon, which indicates a maximum deposition age, is 2014 ± 23 Ma.

Sample KI 25 (Figs. 3 and 7) was collected from the Muyinga Quartzite–Muyinga Formation. Sixty five zircons were analysed and showed Th/U ratios from 0.28 to 4.78. Common lead Pb (f_{206}) was generally below 1% but 6 zircons contained more than 2% and another 5 zircons contained more than 4%. Forty zircons yielded ages 95% concordant in 4 age groupings. These range from 2.79 to 2.62 Ga (20%), 2.47 to 2.4 Ga (10%), 2.14 to 1.93 Ga (20%), 1.90 to 1.83 Ga with one zircon at 1.75 Ga (totalling 45%). The two youngest zircons (5%) were dated 1.42 and 1.41 Ga (Fig. 8d and e). The oldest group of zircons (2.79–2.62 Ga) range in size from 80 to 100 μm with length to width ratios of 2:1 to 1:1. Some of these are subrounded to euhedral and show well-developed oscillatory zoning in CL consistent with a magmatic origin. The youngest two groupings (2.14–1.75 Ga) range in size from 60 to 150 μm with length to width ratios of 2:1 to 1:1 and are subrounded to angular with many euhedral crystals. Many show well-developed concentric zoning in CL consistent with a magmatic origin. The two youngest zircons (1421 ± 37 Ma and 1412 ± 21 Ma) are 100 to 120 μm in size, with a length to width ratio of 2:1 and show poor zonation in CL but are considered as magmatic in origin. These two concordant analyses

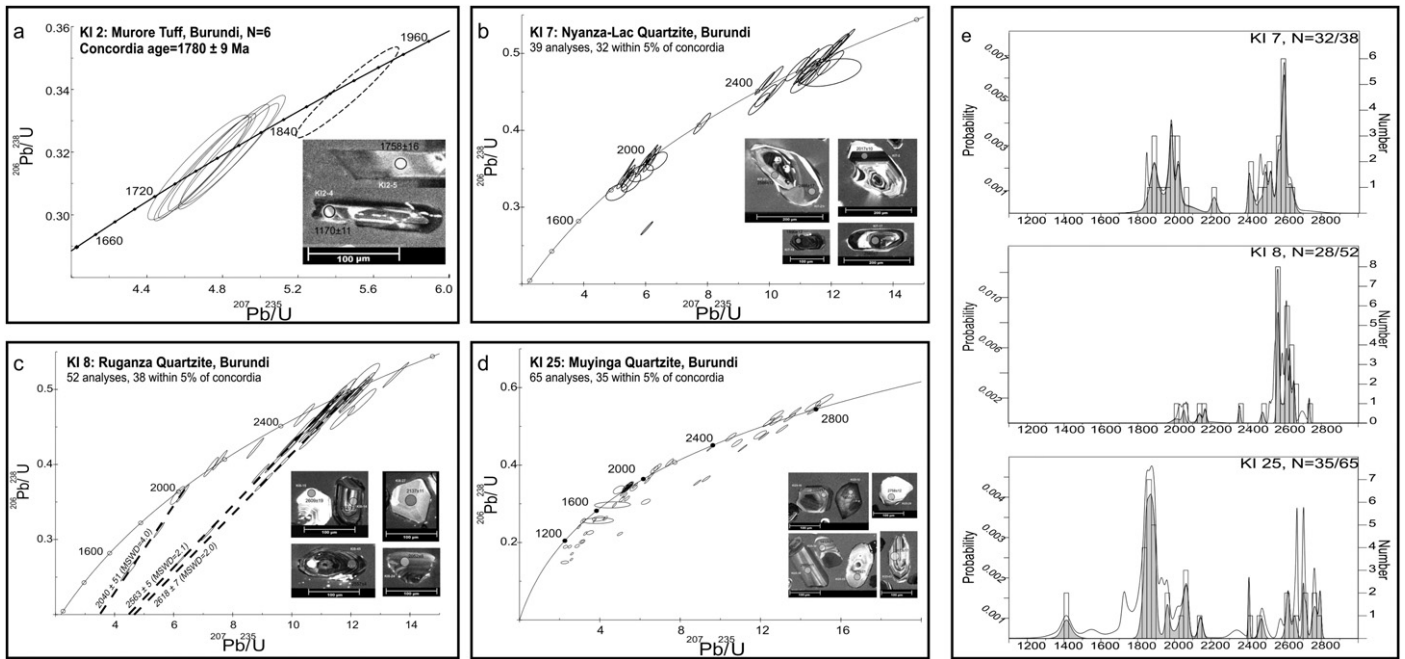


Fig. 8. Single-zircon U–Pb SHRIMP Concordia ages of four analysed samples from Burundi (location: see Fig. 3; stratigraphic position see Fig. 7). (a) KI 2: Murore Tuff (ED), magmatic zircons. (b) KI 7: Nyanza-Lac Quartzite (ED), detrital zircons. (c) KI 8: Ruganza Quartzite (WD), detrital zircons. (d) KI 25: Muyinga Quartzite (WD), detrital zircons. (e) Histogram of samples KI 7, KI 8 and KI 25, showing significant provenance of Archaean and to lesser extent of Palaeoproterozoic detrital material. Maximum age of deposition is given by the small 1.4 Ga peak.

represent the maximum deposition age of the Muyinga Formation (uppermost part of the basal Gikoro Group; Fig. 7). A third, slightly discordant and imprecise analysis of 1380 ± 57 Ma adds further weight to this younger zircon population, whose age overlaps with the c. 1375 Ma emplacement age of the bimodal magmatism of the WD. It is suggested that these three zircons were reworked from a felsic volcanic unit in the Muramba Formation, lithostratigraphically just below the Muyinga Formation, as observed in situ by one of the co-authors (Tack).

5. Discussion: timing of deposition, detrital provenance, basin environment and regional setting

The new lithostratigraphy, geophysical data and provenance analysis support the subdivision of the KAB into two contrasting structural domains (the ED and the WD), introduced by Tack et al. (1994). These confirm the rheologically contrasting boundary zone between the WD (overlying Palaeoproterozoic basement) and the ED (overlying Archaean basement). The identified lithostratigraphic successions are unique in the ED (Kagera Supergroup) and in the WD (Akanyaru Supergroup) and each distinct sedimentary succession has been deposited independently in the respective sub basins under different conditions.

5.1. A first sedimentation period recorded in the ED

Onset of deposition in the KAB is documented in the Kagera Supergroup (ED) and constrained by the emplacement of the Murore felsic tuffs (dated 1780 ± 9 Ma) interlayered with sandstone near the base of the Muyaga Group which is deposited unconformably on the Archaean Tanzania Craton (Figs. 7 and 9). Evolution of the ED started adjacent to the 2100–2025 Ma (Eburnean-age) Ubende-Rusizi Belt (Theunissen et al., 1996; Ring et al., 1997; Sklyarov et al., 1998; Muhongo et al., 2002). Deposition of the 1780 Ma Murore felsic tuffs follows closely the c. 1.88–1.85 Ga volcano-plutonic events that consolidated the NE Congo-Uganda,

Kasai-Angola and Tanzania Archaean Craton (Schandlmeier, 1983; Kabengele et al., 1991; Lenoir et al., 1994; Kapenda et al., 1998).

The uppermost part of the Ruvubu Group in the western sub basin of the ED is intruded by the c.1375 Ma KM mafic and ultra-mafic magmatism, showing that deposition of the complete Kagera Supergroup occurred prior to c. 1375 Ma. The sedimentation age of the Bukoba Group in the eastern sub basin of the ED, is also prec. 1375 Ma (Deblond et al., 2001) but there is no constraint on the base which has not been observed (see Sections 3.1.4 and 3.2).

In the ED, detrital components comprise material only of Archaean and Palaeoproterozoic origin. Oldest detrital zircons range in age from 2.67 to 2.40 Ga (KI 7). These ages are consistent with the age of granitoid lithologies in the nearby Archaean Tanzania Craton, which may be the source of the zircons. The younger detrital zircon group from 2.02 to 1.85 Ga (KI 7) may correspond to ages of granitoids and gneisses of the nearby Palaeoproterozoic Ubende-Rusizi and Ruwenzori Belts and even of the more distant volcano-plutonic Bangweulu Block (De Waele et al., 2006, 2008). The deposits of the Kagera Supergroup can be considered an Eburnean-age molasse.

5.2. A second sedimentation period recorded in the WD

Subsequent deposition in the KAB is found only in the WD with the Gikoro and Pindura Groups of the Akanyaru Supergroup. Note, however, that the base of the complete sedimentary succession in the WD has not been observed (Figs. 7 and 9).

Deposition started sometime after 1420 Ma (felsic volcanic event, sample KI 25; 1420–1380 Ma) but before 1375 Ma (emplacement age of the S-type granitoid rocks) (Figs. 7 and 9). The basin evolution indicates tectonic controls, well-traced by both the depositional and magmatic history. The Pindura Group, predominantly of metapelitic composition, is marked by interlayered volcanic episodes (mafic tholeiitic amygdaloidal basalts overlain by a sequence of felsic lavas –both effusive and explosive facies) (Figs. 7 and 9). This bimodal volcanism is considered the surface

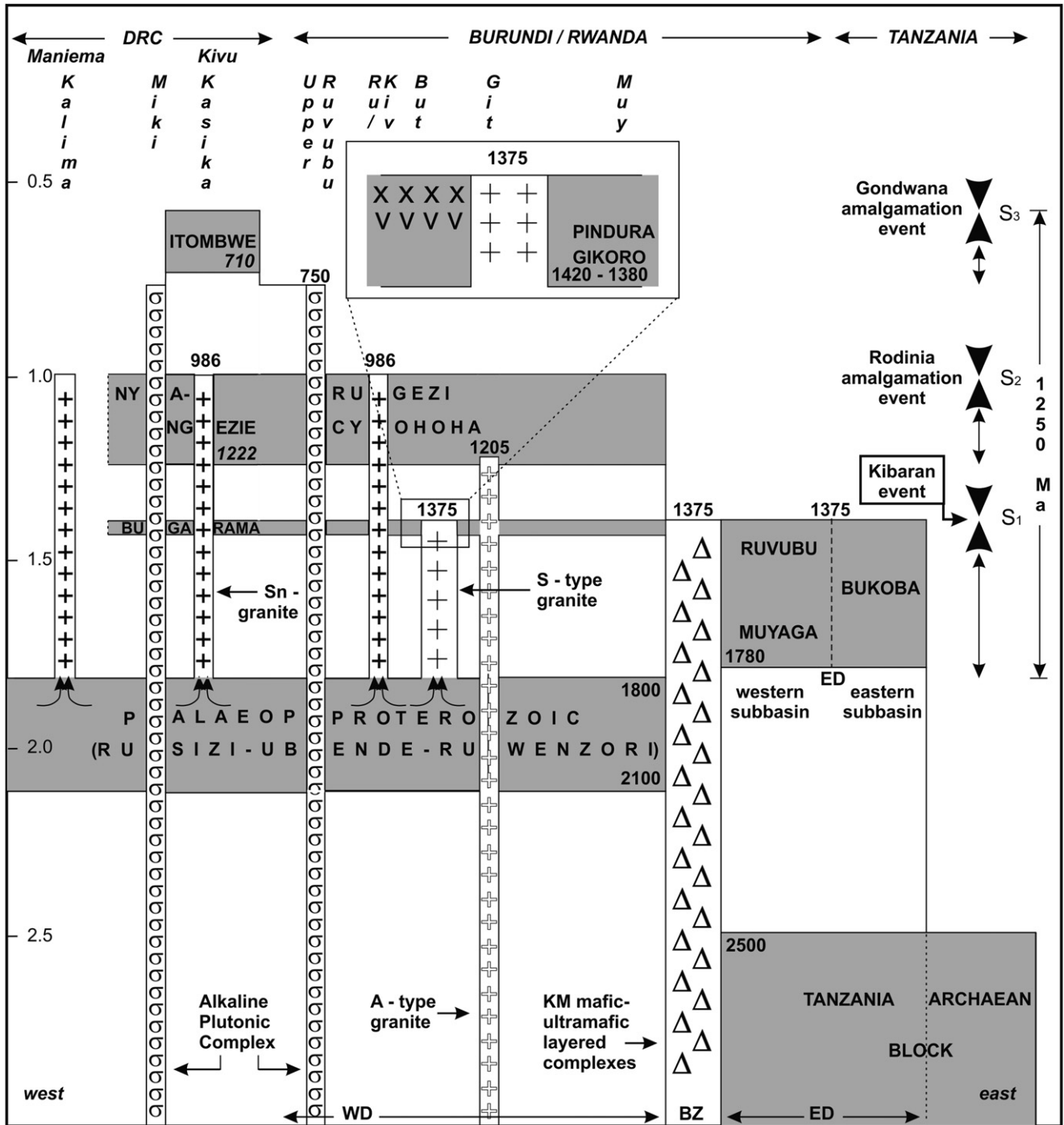


Fig. 9. Synthetic chronostratigraphic reconstruction of the KAB (WD – BZ – ED) within a regional geological setting, based on recent available ages from literature and this paper. X-axis corresponds to schematic geological W–E cross-section at about 3°S (not at scale); see also Figs. 2, 3 and 6. Y-axis is time scale in Ga. Top line refers to localities used in tekst: Kalima (Maniema region); Miki (Kivu region); Upper Ruvubu (Burundi); 750 Ma alkaline complexes; Kasika (Kivu region); Ru/Kiv – Ruhembe and Kivuvu (Burundi); 968 Ma Sn-coltan pegmatites; But. – Butare (Rwanda); 1982 Ma orthogneiss of Eburnean-aged basement; Git. – Gitega (Burundi); 1205 Ma A-type granitoids; Muy. – Muyinga (Burundi); location of sample KI 25. Right-hand axis: time-frame of major regional events having affected the KAB and resulting deformational fabric in the KAB metasediments: S1: development of a pervasive S₁-fabric (parallel to bedding S₀); S2: development of a discrete S₂-fabric; S3: brittle reactivation in WD of earlier thrust slices.

representative of the 1375 Ma bimodal Kibaran event (Tack et al., 2010).

In the WD, detrital zircons range in age from 2.73 to 2.48 Ga (KI 8) and 2.79 to 2.62 Ga (KI 25). These ages are consistent with the age of granitoid lithologies in the nearby Archaean Tanzania Craton, which may be the source of the zircons. Younger detrital zircon groups from 2.07 to 2.01 Ga (KI 8), and from 2.47 to 1.75 Ga

(KI 25) may correspond to ages of granitoids and gneisses of the nearby Palaeoproterozoic Ubende-Rusizi and Ruwenzori Belts and maybe also of the more distant volcano-plutonic Bangweulu Block (De Waele et al., 2006, 2008). The large contribution of Palaeoproterozoic components in the WD strengthens the view that the WD is underlain by Palaeoproterozoic basement, as has been confirmed in the Butare region of SW Rwanda (Tack et al., 2010).

5.3. A third sedimentation period documented in the WD

After the 1375 Ma bimodal Kibaran event (Tack et al., 2010), a third sedimentation period at 1222 Ma is documented by detrital zircons from the base of the Nya-Ngezie unit in the Kivu-Maniema area of the DRC (Villeneuve and Chorowicz, 2004) (Figs. 7 and 9). This unit can be correlated along trend with the Cyohoha and Rugezi Group in the WD, i.e. the upper part of the Akanyaru Supergroup (Figs. 7 and 9). The Nya-Ngezie unit rests disconformably on the Bugarama unit (Villeneuve, 1980; see Section 3.1.5) that can likewise be correlated with the Gikoro and Pindura Groups of the WD.

While no disconformity exists at the base of the Cyohoha Group in the WD, a stratigraphic break is also suggested in Rwanda at this level (see Section 3.2). The c. 155 m.y. interval between the intrusion of the 1375 Ma bimodal Kibaran event at a depth of ± 15 km into the lower part of the Akanyaru Supergroup, and the onset of deposition at 1220 Ma of the upper part of this Supergroup, provides ample time for an depositional or erosional hiatus.

The break in the sequence also explains why the pervasive extensional S_1 -fabric (typically sub parallel to bedding surfaces S_0), in the lower Gikoro and Pindura Groups (Theunissen, 1988, 1989; see Section 3.2) is absent from the higher units. Renewed subsidence in the WD around 1220 Ma may have been triggered by reactivation of N–S trending shear zones, evident in Burundi as the alignment of small A-type granitoids bodies emplaced at c. 1205 Ma (Tack et al., 2010) (Figs. 4 and 9).

5.4. A gradual depositional polarity from E to W during the greater part of the Proterozoic

The Itombwe “Syncline” in the vicinity of Bukavu town (Fig. 6, inset 1 and 2) is a narrow, N–S elongated structure containing sedimentary successions, including diamictites (Itombwe Supergroup; Villeneuve, 1980, 1987; Walemba and Master, 2005) which rests unconformably on either Palaeoproterozoic or Mesoproterozoic basement (Lepersonne, 1974; Cahen et al., 1979). Walemba and Master (2005) discuss these successions nearby Nya-Ngezie (Bukavu; Fig. 6), where the basal conglomerate of the Nya-Kasiba Group (lowermost unit of the Itombwe Supergroup) (Figs. 7 and 9) contains pebbles of the Kasika tin-granite (Cahen and Ledet, 1979; Cahen et al., 1979; Villeneuve, 1987). The Kasika tin-granite, dated 986 Ma (Tack et al., 2010), confirms the Neoproterozoic age of the Itombwe Supergroup. Detrital zircons from the basal conglomerate gave a maximum deposition age of c. 710 Ma (Villeneuve, pers. comm. referring to unpublished SHRIMP-data of Kampunzu and Armstrong).

This age marks a Neoproterozoic sedimentation period within the KAB area and illustrates that basin evolution in the WD is not limited to only the Mesoproterozoic era. Likewise, remnants of similar but much smaller basins exist in Rwanda and Burundi (e.g. the Karamba, Miyove and Gisakura Formations in Rwanda, the Mikiko Formation in Burundi), all part of the uppermost Rugezi Group which has proven difficult to incorporate into the formal Akanyaru Supergroup stratigraphy (Baudet et al., pers. comm.).

The KAB thus documents a long-lived period of intracratonic intermittent depositional activity showing a recurrent subsidence trend controlled by tectonic activity moving with time from E to W. In the WD, this E to W sedimentary polarity can be correlated – and therefore must be geodynamically related – to a similar polarity trend in extensional magmatism, characterised successively by the 1375 Ma bimodal Kibaran event, the local emplacement of the 1205 Ma A-type granites as well as of the 750 Ma alkaline plutonic complexes (Fig. 9).

During this long-lived Proterozoic period, spanning about 1250 m.y. from the late Palaeoproterozoic (1.8 Ga) to the end of the Neoproterozoic (542 Ma), the KAB is marked by prolonged

intracratonic stability with intermittent episodes of extensional (transtensional) activity of variable intensity. These were interrupted twice by short-lived phases of compression (at 1.0 Ga and 550 Ma) interpreted to be possibly related to Rodinia and Gondwana amalgamations.

The remarkable similar detrital fingerprints of the successions of the ED and WD (Fig. 8e) with supply from the neighbouring Archaean Tanzania Craton and the Palaeoproterozoic Ubende-Rusizi and Ruwenzori Belts respectively, suggest that since Late Palaeoproterozoic times their rheologically contrasting basement domains were in an adjacent position. The detrital fingerprint of some quartzites in the WD may reflect reworking of older sedimentary sequences within the KAB itself.

6. Regional correlations

On a regional geological map of central Africa, Mesoproterozoic formations appear to be limited to the eastern and southeastern side of the Central Congo Basin. They comprise the Karagwe-Ankole Belt (KAB), the Kibara Belt of N. Katanga (KIB), the Irumide and Southern Irumide Belts (Zambia), and formations on the Bangweulu Block (Zambia) as well as strike-slip basins within the Palaeoproterozoic Ubende Belt (e.g. Itiaso Group) in Tanzania (Fig. 10).

Similarities in their terrigenous sequences must reflect basin histories recording similar regional responses to major geodynamic events, while differences probably reflect more local responses – in a particular basin or in some basins – to these geodynamic conditions.

6.1. Similarities

6.1.1. 1.88–1.78 Ga period

The first sedimentation period in the KAB is dated at 1.78 Ga (crystallisation age of the Murore Tuff at the base of the Kagera Supergroup). During this period shallow-water quartzites and pelites with detrital modes of 2.7–2.5 Ga and 2.0–1.8 Ga were deposited (see Section 4.1).

A similar succession, the Muva Supergroup, south of the KAB in Zambia, rests on the Bangweulu Block (Fig. 10, samples MA6 and KAS) and is present in the Mesoproterozoic (northern) Irumide Belt of Zambia (Fig. 10, sample IL14). Tuffs at the base of the Muva Supergroup place onset of deposition between 1.88 and 1.85 Ga (De Waele and Fitzsimons, 2007), and show similar detrital age patterns as the KAB successions. The significant Archaean mode of 2.7–2.5 Ga zircons in the Kagera Supergroup successions of the ED, with its source in the neighbouring Tanzania Craton, is nearly absent within the Muva sedimentary succession (De Waele and Fitzsimons, 2007), in keeping with its distant location on the far south side of the Palaeoproterozoic Ubende Belt.

Lithologies within the Ubende-Rusizi Belt document peak metamorphism between 2.1 and 2.0 Ga (Theunissen et al., 1996; Ring et al., 1997; Sklyarov et al., 1998; Muhongo et al., 2002), exhumation of the Belt in the time interval 1.95–1.85 Ga (Boven et al., 1999) and plutono-volcanic events at ca. 1.88–1.85 Ga (Schandelmeier, 1983; Kabengele et al., 1991; Lenoir et al., 1994; Kapenda et al., 1998; Reddy et al., 2003). These ages match detrital modes in the Kagera and Muva successions (Fig. 10). The data demonstrate the large geographical extent, both N and S of the Ubende-Rusizi Belt, and considerable time-span of sedimentary successions (i.e. 100 m.y. between 1.88–1.78 Ga) deposited immediately after the Eburnean-age orogeny in different independent basins, and largely derived from these Palaeoproterozoic Belts.

6.1.2. 1.42–1.37 Ga period

The second sedimentation period in the KAB is recorded at 1.42–1.37 Ga in the Akanyaru Supergroup (see Section 4.2). The

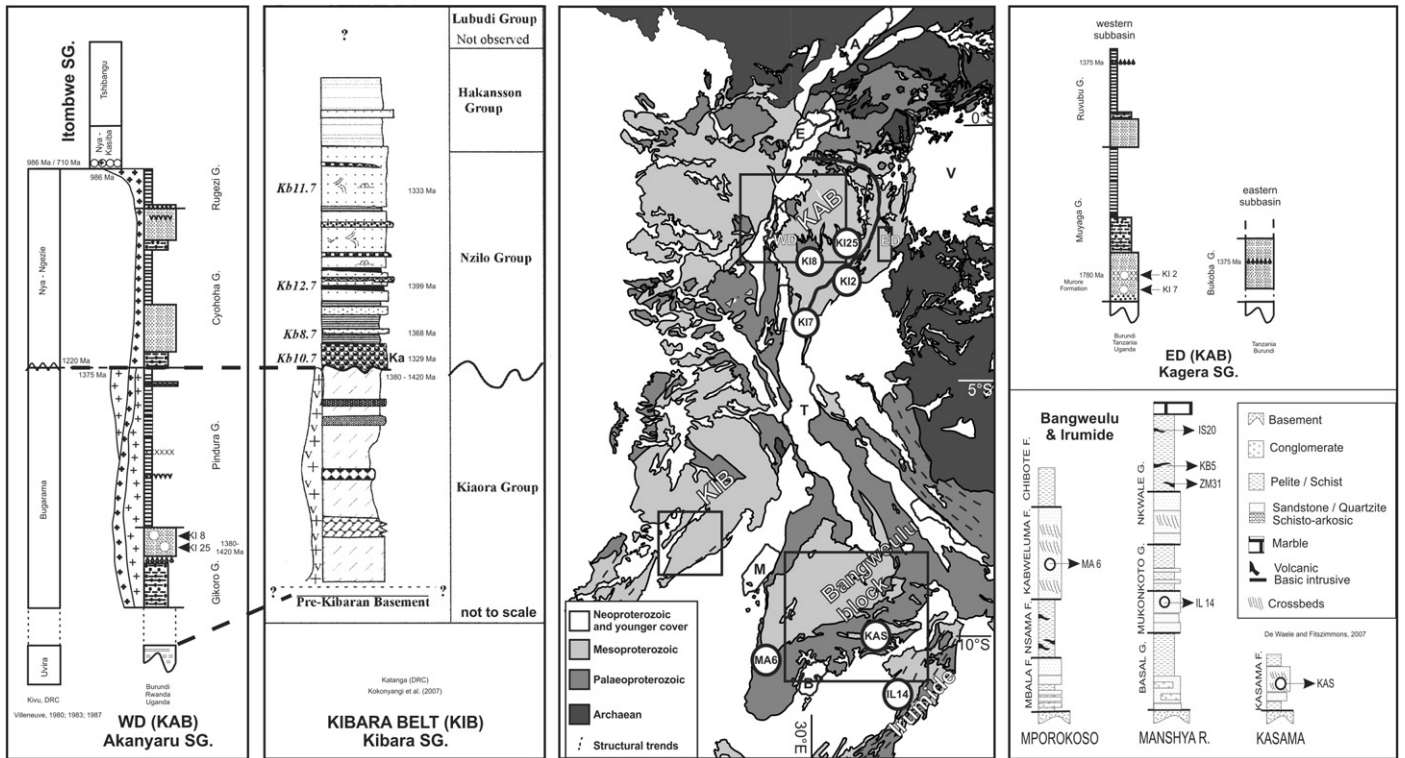


Fig. 10. Lithostratigraphical correlations between the Karagwe – Ankole Belt, Kibara Belt, Bangweulu Block and Northern Irumide Belt. Centre: regional geological setting (simplified from Fig. 6) showing the location of the considered regional units. Squares refer to logs left and right. *Left:* lithostratigraphical columns for the WD of the KAB (this work) versus the KIB (square degree of Mitwaba, mapped by Kokonyangi et al. (2001, 2004, 2005, 2006, 2007); highlights partly similar Mesoproterozoic evolution. *Right:* lithostratigraphical columns for the ED of the KAB (this work) versus the columns for the Bangweulu Block and Northern Irumide Belt (after De Waele and Fitzsimons, 2007); highlights the similar Late Palaeoproterozoic molasses-deposit setting of these units.

age clusters of 2.7–2.5 Ga and ca. 1.8 Ga are consistent with supply from the neighbouring Tanzania Craton and adjacent Late Palaeoproterozoic Ubende-Rusizi Belt, but may also reflect reworking of underlying older sedimentary sequences.

The Kasama Formation on the Bangweulu Block (Fig. 10) was suggested by Andersen and Unrug (1984) to be derived from reworking of the underlying Mporokoso Group, based on palaeocurrent directions, pebble size variations and maturity of the quartzites. The youngest concordant zircon of the Kasama Formation yielded a $^{207}\text{Pb}/^{206}\text{Pb}$ maximum deposition age of 1.43 Ga, similar to that of the Muyinga Quartzite in the WD.

For the Mitwaba area in the Kibara Belt (KIB) in N. Katanga, Kokonyangi et al. (2001, 2005, 2006, 2007) have redefined the Kibara Supergroup (after Cahen et al., 1984) with four lithostratigraphic units, from base to top respectively, the Kiaora, Nzilo, Hakansson and Lubudi Groups (Fig. 10). S-type granitoid rocks associated with mafic-intermediate intrusive rocks are coeval at c. 1.39–1.38 Ga (Kokonyangi et al., 2004, 2005), i.e. a similar Mesoproterozoic age pattern as for the WD in the KAB. Only the lowermost Kiaora Group is intruded by these intrusive rocks.

6.1.3. 1.0 Ga period

The uppermost limit of the third sedimentation period in the KAB is given by the U–Pb SHRIMP 986 Ma emplacement age of the Kasika tin-granite in the Cyohoha-Rugezi Groups (Tack et al., 2010; Fig. 10). Similarly in the Mitwaba area in the Kibara Belt (KIB), Kokonyangi et al. (2001, 2005, 2006, 2007) document a minimum age constraint for the Nzilo, Hakansson and Lubudi Groups given by the emplacement of tin-granites dated c. 1.0–0.95 Ga (Kokonyangi et al., 2004, 2006) and by the 1080 Ma age of the local metamorphic overprint in the Mitwaba area quoted as “corresponding to the climax of the Kibaran deformation” (Kokonyangi et al., 2006).

6.2. Differences

6.2.1. Eburnean-age molasse deposits and boundary zone

The WD – boundary zone – ED structure of the Karagwe – Ankole Belt is a unique feature of this belt.

In the KIB of N. Katanga, Eburnean-aged foreland deposits (comparable to the ED of the KAB) are absent. The sedimentary record appears to comprise equivalents of the WD Akanyaru Supergroup of the KAB, while molasse deposits are found only 200–300 km further to the E on the Bangweulu Block in Zambia (see Section 6.1; Fig. 10).

An equivalent of the mafic-ultramafic Kabanga–Musongati alignment (KM) of layered Bushveld-type complexes forming the boundary zone of the KAB is absent in the KIB.

6.2.2. Different sedimentation breaks between 1.37 and 1.0 Ga

The stratigraphic record in the WD of the KAB indicates a c. 155 m.y. depositional hiatus (see Section 3.2) between the lower part of the Akanyaru Supergroup intruded by the 1375 Ma bimodal Kibaran event and the overlying the Nya-Ngezi unit, which has a maximum deposition age of c. 1220 Ma (Figs. 9 and 10).

In the Mitwaba area in the Kibara Belt (KIB), the base of the Nzilo Group rests disconformably on the Kiaora Group and the c. 1.39–1.38 Ga intrusive rocks. The Nzilo Group is marked by a conglomerate, the Kataba Conglomerate (Ka), which contains reworked Kiaora Group sediments and intrusives. Detrital zircon dating of 4 samples (Kokonyangi et al., 2007; Fig. 10) give a 1329 Ma maximum deposition age for the Nzilo Group. This indicates a depositional hiatus between the lowermost Kiaora and overlying Nzilo Group not exceeding c. 50 m.y., shorter than the c. 155 m.y. depositional hiatus suggested in the KAB (see Section 5.3).

A different Mesoproterozoic basin history for the KAB and the KIB after 1375 Ma is also expressed by the differing lithologic successions in the Nzilo (KIB) and Cyohoha-Rugezi (KAB) Groups, Fig. 10).

6.2.3. Other Mesoproterozoic basins in the area

Within the Ubende-Rusizi basement rise, local Mesoproterozoic strike-slip basins have been described (Klerkx et al., 1998), each with their own unique lithostratigraphic and geodynamic characteristics (e.g. Itiaso Group), and different from those of the KAB or the KIB (Geology and Mineral map of Tanzania, 2008).

7. The concept of a proto-Congo Craton assembly at 1.8 Ga

The Karagwe-Ankole, Kibara, Bangweulu and Irumide successions appear to have experienced comparable geodynamic basin evolution during the Proterozoic with periods of interruption of deposition, erosion and magmatism. The time-span, regional distribution and depositional character of the successions suggest the existence of long-lived shallow-water intracratonic basins. Sedimentation started between 1.88 and 1.78 Ga, and represents the deposition of Eburnean-age molasse, followed by periods of Mesoproterozoic sedimentation, during which the earlier molasse may have been partially reworked. Such long-lived basin evolution is comparable to the Neoproterozoic Central Australian basins (Powell et al., 1994).

The close match and regional distribution of c. 1.8 Ga sedimentary sequences along the eastern side of the Congo River Basin, suggest that the Tanzania, NE Congo-Uganda, Bangweulu and Kasai Blocks were amalgamated along the Ubende-Rusizi Belt and Ruwenzori Fold Belt, and formed part of a coherent landmass in Late Palaeoproterozoic times (Fig. 11a). Broad similarities in both age and sedimentary character have also been observed in pre-Kibara successions further west on the Angola Block – Chela Group (Torquato and Fogaça, 1981; Pereira et al., 2011) and even in the Espinhaço – Chapada Diamantina Groups on the São Francisco Block in Brazil (Pedreira and De Waele, 2005; Danderfer et al., 2009; Chemale-Junior et al., 2012; Pedrosa-Soares and Alkmin, 2011; Fig. 11a). This suggests that, as a result of Eburnean-age collisional orogeny during the Columbia (Nuna) amalgamation (De Waele et al., 2006, 2008; Delor et al., 2008; Noce et al., 2007; Pinna et al., 1996), all these Archaean nuclei were welded together around 2.1 Ga. Widespread basin deposition commenced from about 1.8 Ga.

We suggest that the assembled landmass formed the proto-Congo Craton (Fig. 11a; Fernandez-Alonso et al., 2011). Since the Late Palaeoproterozoic, this proto-craton stabilised and remained a united entity (Tack et al., 2006, 2008), which underwent repeated intracratonic transtensional tectonomagmatic events (Tack et al., 2010, 2011; Delvaux et al., 2011) but not breakup, drifting or the formation of juvenile oceanic crust. Rodinia and Gondwana orogenic events are considered to have occurred along the margins of the proto-Congo craton. Only since the opening of the south Atlantic ocean in Cretaceous times, did a minor portion (the westernmost Sao Francisco Block) become separated.

The KAB reflects a very long aulacogene history in part of the proto-Congo craton with intermittent periods of sedimentation and/or magmatism (Fig. 9). We suggest that fundamentally different geometries and rheologies of the KAB's basement on both sides of the boundary zone account for the specific exogenic and/or endogenic geological processes recorded during the Proterozoic in the WD as opposed to the ED (Tack et al., 2010). Since 1.78 Ga, repeated reactivation of structures in the Ubende-Rusizi basement rise (Klerkx et al., 1998) controlled volcano-sedimentary basin development in the KAB during the Proterozoic. Basin infill,

comprising intermittent subsiding shallow-water deposits possibly with bimodal volcanism, shifted from the E to the W. Magmatism culminated at c. 1375 Ma with the Kibaran event (coeval bimodal magmatism) followed by relatively minor intracratonic magmatic events at c. 1205 Ma (A-type granitoids), c. 985 Ma (tin-granites) and c. 750 Ma (alkaline complexes, some with carbonatites, see Tack et al., 1984, 1996; Kampunzu et al., 1997; Mbete et al., 2004).

The Kibaran magmatic event indicates the final consolidation of this part of the proto-Congo Craton, as subsequent events in Central – Eastern Africa (see e.g. Tack et al., 2002a, 2010; Fig. 9) have not disturbed the craton's integrity.

8. Basin closure: two short-lived far-field compressional events in the KAB

In the last decades, two contrasting geodynamic models for the KAB (and the KIB) have been proposed: an intraplate extensional setting with bimodal magmatism followed by a series of compressional events (Klerkx et al., 1984, 1987) versus a convergent setting along an active continental margin (Kampunzu et al., 1986; Rumvegeri, 1991). Both models implicitly considered that the Kibaran orogeny occurred in Central Africa in Late Mesoproterozoic times (1.4–1.0 Ga) and had a protracted character with significant magmatic episodes from c. 1370–1310 Ma (Cahen et al., 1984) up to 1180 Ma (Klerkx et al., 1984, 1987).

Most recent regional evidence related to the KAB (Tack et al., 2010 and references therein) indicates that the KAB did not result from the closure of an ocean basin and subsequent continent-continent collision. The KAB, and also the KIB, developed separately (see Section 6) under intraplate conditions within the already consolidated Archaean-Palaeoproterozoic proto-Congo Craton.

With new age constraints for the same samples of Cahen et al. (1984) and Klerkx et al. (1984, 1987), Tack et al. (2010) introduced a single anorogenic prominent 1375 Ma Kibaran tectonomagmatic event with intracratonic, i.e. intraplate transtensional emplacement of a bimodal magmatic province. This event is not related to any orogenic cycle at plate edges. It implies that the recorded compressional deformation phase(s) in the KAB postdate the Kibaran event and the deposition of the younger Upper Mesoproterozoic (i.e. post 1375 Ma) and Neoproterozoic successions described in the WD (Fig. 9).

A first compressional event acting on the KAB reflects a far-field effect of a global orogenic event external to the proto-Congo Craton and marked by the collisional Irumide and Chipata-Tete (or Southern Irumide; Fig. 11b) Belts (Johnson et al., 2006, 2007; De Waele et al., 2006, 2008, 2009; Li et al., 2008) during Rodinia amalgamation at 1.0 Ga. The morpho-structural response in the KAB (and the KIB) to the distant Irumide Orogen, was accommodated by displacement along the Ubende-Rusizi Belt (Tack et al., 2006, 2008; Fernandez-Alonso et al., 2009, 2011) (Fig. 11b). In the KAB, the metasedimentary rocks of the WD basin were folded and thrust as a result of reactivation of structures in the underlying Palaeoproterozoic basement (Theunissen, 1988, 1989) and developed a discrete (for the most oblique) S₂-fabric, postdating the S₁-fabric which is related to the 1375 Ma Kibaran event (see Section 5.3). The metasedimentary rocks of the ED, overlying Archaean basement, remained generally undisturbed. Post-compressional relaxation (i.e. post-S₂) gave rise to the emplacement of the post-Kibaran Sn-metallogenic province (new SHRIMP-age of tin-granite emplaced in the WD at ca. 986 Ma (Tack et al., 2010; Dewaele et al., 2011).

Subsequently during Gondwana amalgamation at 550 Ma, a second E to W directed compressional event affected the KAB as a far-field effect of the distant East African Orogen (Fig. 11c) (Rossetti et al., 2007; Dewaele et al., 2011; Kabete et al., 2012). In the southern part of the WD, the specific indenter palaeogeography

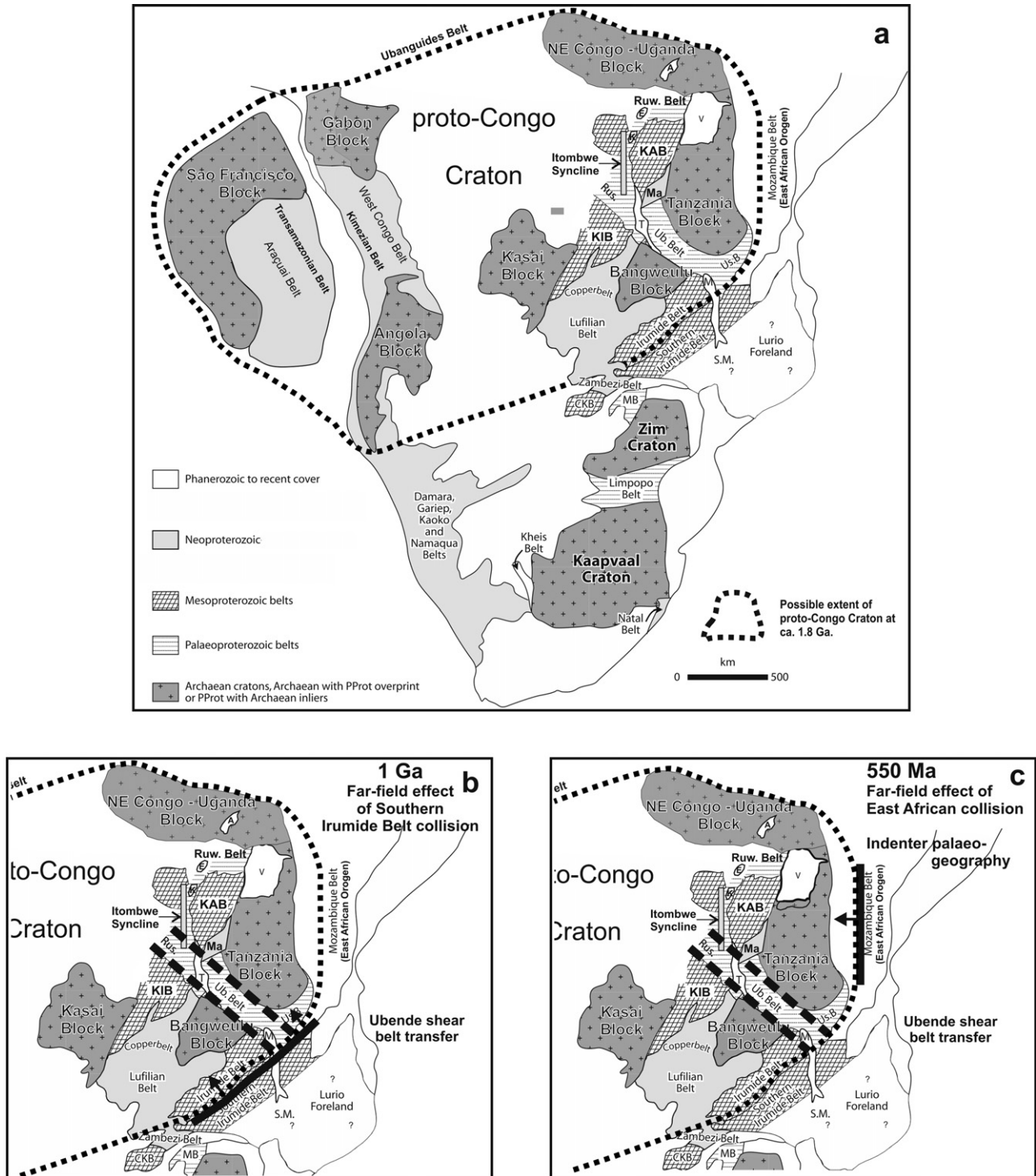


Fig. 11. Regional setting of the Mesoproterozoic units within a proto-Congo Craton (modified from De Waele et al., 2008). (a) Intracratonic basin formation under transtensional regime. Starts at 1780 Ma in the Karagwe – Ankole Belt (KAB) and culminates at 1375 Ma with the Kibaran bimodal magmatic event – also recorded in the Kibaran Belt (KIB) – responsible for development of a pervasive S_1 -fabric in the metasediments of WD in the KAB (parallel to original bedding S_0). (b) First compressional event at 1.0 Ga. Basin closure of the KAB results from an intraplate far-field effect of Rodinia amalgamation along the Southern Irumide Belt. Note role of Ubende-Rusizi shear Belt accommodation. This compressional event is responsible for the general fold-and-thrust-belt geometry of the KAB with development of a discrete S_2 -fabric. The 986 Ma Sn-granite (Tack et al., 2010) and related Sn-mineralisation were emplaced during regional relaxation in parts of the WD (of the KAB) shortly after compression. (c) Second compressional event at 550 Ma. Intraplate far-field effect of Gondwana amalgamation along the Eastern African Orogen, resulting in the present-day morpho-structural trend of the KAB. A strong but discrete N–S Pan African tectonic overprint in southern part of the WD is due to the indenter palaeogeography of the Archaean Tanzania Craton squeezing the Proterozoic rocks. This gives rise in the WD to brittle reactivation of (earlier) thrust slices (S_3), (partial) isotopic resetting of rocks and mineralisations, emplacement of Au-mineralisation in quartz veins, while steep folding (and thrusting) of the Neoproterozoic Itombwe basin gives rise to the Itombwe “Syncline”. Note that the importance of this Pan African event has often been unrecognised or strongly underestimated. The timing of the events is illustrated in Fig. 9, right hand side.

of the Archaean Tanzania Craton (Fig. 4) gave rise to a pronounced squeezing of earlier structures (Fig. 3). As a result, N–S trending thrust sheets and imbricate structures developed together with discrete isotopic resetting and post-compressional (i.e. post-S₃) c. 530 Ma emplacement of late Pan-African Au-mineralisation (Brinckmann et al., 2001; Walemba, 2001; Walemba et al., 2004; Dewaele et al., 2011). The N–S elongated Neoproterozoic Itombwe basin became steeply folded forming the Itombwe “Syncline” (see Section 3.1.5). This strong but discrete N–S Pan African overprint has generally been underestimated or even overlooked in literature.

9. Conclusions

Our new results related to basin evolution, timing of deposition and provenance of the sedimentary record give additional weight to the recent redefinition of the KAB and the KIB, forming two distinct Belts respectively north and south of the Palaeoproterozoic basement high of the Ubende – Rusizi Belts.

Only the redefined 1375 Ma Kibaran tectonomagmatic event is recorded in both the KAB and the KIB; likewise the sedimentary and volcanic record of the KAB in the period 1.42–1.37 show similarities with those described for the KIB. However, the WD – boundary zone – ED build-up of the KAB is a unique feature. In the KIB, an Eburnean-aged molasse in an ED-type domain or an equivalent to the mafic–ultramafic KM alignment of layered Bushveld-type complexes forming the boundary zone are lacking. A different post-1375 Ma Mesoproterozoic and Neoproterozoic basin evolution as well as compressional history is expressed for the KAB and the KIB by the differing lithologic successions and deformational histories. The discontinuity between the KAB and the KIB is further marked by the occurrence within the Ubende-Rusizi Belts basement high of local Mesoproterozoic strike-slip basins, with their own unique lithostratigraphic and geodynamic characteristics (e.g. Itiaso Group), which differ from those of the KAB or the KIB.

In the Karagwe-Ankole Belt (KAB) the new lithostratigraphy takes into account two rheologically contrasting structural domains, i.e. the Eastern Domain (ED; with Archaean basement) separated from the Western Domain (WD; with Palaeoproterozoic basement) by a boundary zone, comprising the Kabanga–Musongati (KM) alignment of Bushveld-type mafic–ultramafic intrusions. Volcanic and detrital U–Pb SHRIMP zircon data for the ED and the WD provide new constraints on the timing of deposition and on the detrital provenance of the sedimentary sequences in both domains.

In the ED, (in E Burundi, NW Tanzania and SW Uganda), the Kagera Supergroup includes two adjacent sub basins separated by a fault that may reflect some palaeogeographic setting. Each has its own lithostratigraphic column: (1) the western sub basin contains the Muyaga and overlying Ruvubu Groups (siliciclastic rocks with interlayered volcanic rocks), and (2) the eastern sub basin contains the former Neoproterozoic Bukoba Group (siliciclastic rocks). Onset of deposition of the Kagera Supergroup is constrained by the emplacement of the Murore felsic tuff of 1.78 Ga interlayered near the base of the Muyaga Group (unconformably overlying the Archaean Tanzania Craton). Deposition of the complete Kagera Supergroup occurred before 1.37 Ga (emplacement of KM intrusions). Detrital components comprise material only of Archaean and Palaeoproterozoic origin, consistent with derivation from the nearby Archaean Tanzania Craton and Palaeoproterozoic Ubende – Rusizi and Ruwenzori Belts. The deposits of the Kagera Supergroup have to be considered an Eburnean-age ‘molasse’.

In the WD (in Rwanda, W Burundi and SW Uganda), the Akanyaru Supergroup includes respectively (from bottom to top), the Gikoro, Pindura, Cyohoha and Rugezi Groups (greenschist- to amphibolite facies metasedimentary rocks and subordinate

inter-layered metavolcanic units). Deposition started in the WD sometime after 1.42 Ga (felsic volcanic event) but before 1.37 Ga (emplacement age of the S-type granitoid rocks). The bimodal volcanism interlayered in the Pindura-Gikoro Groups is considered the surface representative of the 1375 Ma ‘Kibaran’ event (Tack et al., 2010). The bulk of the detrital zircons of the WD are of Archaean and Palaeoproterozoic age, consistent with derivation from the nearby Archaean Tanzania Craton and Palaeoproterozoic Ubende-Rusizi and Ruwenzori Belts (and possibly of the more distant volcano-plutonic Bangweulu Block). The large contribution of Palaeoproterozoic components in the WD strengthens the view that this domain is underlain by Palaeoproterozoic basement, as has been confirmed in the Butare region of SW Rwanda (Tack et al., 2010). It also supports the concept that part of the Akanyaru Supergroup sediments consists of reworked Eburnean-aged molasse.

A later sedimentation period in the WD at 1222 Ma is documented by detrital zircons from the base of the Nya-Ngezie unit in the Kivu-Maniema area (in DRC), which can be correlated with the Cyohoha-Rugezi Groups, i.e. the upper part of the Akanyaru Supergroup. Finally, onset of a Neoproterozoic sedimentation in the local Itombwe basin (in DRC) is constrained at 710 Ma.

The KAB documents a long-lived period of intracratonic intermittent depositional activity (with periods of interruption of deposition, erosion and magmatism) showing a recurrent subsidence trend controlled by structural activity moving with time from E to W. In the WD, this E to W sedimentary polarity can be correlated – and therefore must be geodynamically related – to a similar polarity trend in extensional magmatism (characterised successively by the 1375 Ma bimodal ‘Kibaran’ event, the local emplacement of the 1205 Ma A-type granites and the double alignment of 750 Ma alkaline plutonic complexes). The E–W sedimentary polarity is even further evidenced when also the 1.8 Ga molasse-type deposits of the ED are taken into account.

On a regional scale, the KAB sequences suggest a comparable and prolonged geodynamic basin evolution, not only with the sequences of the relatively close Kibara (KIB), Bangweulu Block and Northern Irumide Belts but even with more distant sequences located in SW Angola and E Brazil. Since deposition of Eburnean-aged molasse, the 1250 my time-span, regional distribution and sedimentological character of all these sequences point to the existence until the end of the Proterozoic of various long-lived shallow-water intracratonic basins within an already previously amalgamated coherent landmass. We postulate that this landmass formed the ‘proto-Congo Craton’, which since the Late Palaeoproterozoic had stabilised and remained a united entity. Only since the opening of the south Atlantic ocean in Cretaceous times a minor portion (the westernmost Sao Francisco block of E Brazil) became separated.

The long-lived aulacogene history of the KAB within the proto-Congo Craton, with intermittent episodes of extensional (transtensional) regime of variable intensity, including the prominent 1375 Ma “Kibaran” event (giving the S1-fabric, Bushveld-type mineralisation in the KM alignment), is interrupted only twice by short-lived compressional deformation reflecting far-field effects of global orogenic events, external to the proto-Congo Craton. The first event at 1.0 Ga (giving the S2-fabric, tin-granite mineralisation as a result of post-compressional relaxation) affects both KAB and KIB and is ascribed to Rodinia amalgamation, here expressed as far-field effect from the Southern Irumide collisional Belt of Zambia. The second event at 550 Ma results from Gondwana amalgamation and, in the KAB, is the far-field and combined effect of both the East African Orogen (EAO) and the indenter paleogeography of the Archaean Tanzania Craton. As a result, it develops a strong but discrete N–S Pan African overprint (giving the S3-fabric, gold mineralisation as a result of post-compressional relaxation), which has generally been underestimated or even overlooked in the literature.

10. Final considerations

The term “Complexe des Kibara” and “Système des Kibara” was introduced by Robert (1931) and referred to a (meta)sedimentary sequence (a Supergroup in present-day terminology), studied in the Kibara Mountains type locality in N Katanga region (DRC). As the deformed and intruded rocks displayed a physiographic NE–SW trend, the term “Kibaran belt” (“chaîne Kibarienne”) was used to refer to the result of mountain-building processes following a geosyncline episode (the “Kibaran”), responsible for the Kibara Mountains.

Later, the concepts of unconformity, orogenic cycle and orogeny became linked to the “Kibaran”. With progress in radiometric dating (1960-ies), “syn-orogenic” (Kibaran) granites were distinguished from “post-orogenic” tin granites. Culmination of the “Kibaran orogeny” was dated at 1370–1310 Ma (Cahen et al., 1984). With introduction of plate tectonics (late '60-ies), the concepts of a Kibaran orogenic cycle and orogeny were expanded to include the Wilson cycle terminology, implicitly linking orogeny to subduction-collision processes at plate edges. Some geologists considered a protracted “Kibaran orogeny”, with several phases between 1370 up to the 970 Ma tin granites (spanning 400 Ma!). More recently the concepts of supercontinent cycles were developed with for this part of the world, the “collisional orogeny” related to Rodinia amalgamation at 1 Ga, closing the Mesoproterozoic Era.

Our work now dramatically changes the views of the geodynamic evolution of the “Kibaran”. No longer the result of a Wilson-style orogenic event, the former “Kibaran Belt” is now considered to consist of two distinct belts: the Karagwe-Ankole Belt and the Kibara Belt, located respectively N and S of the NW–SE trending Palaeoproterozoic basement extension. Both belts are the result of a long-lived intracratonic shallow basin history within a proto-Congo Craton with intermittent periods of depositional activity (interruption of deposition, erosion) and magmatism (e.g. 1375 Ma emplacement under extensional regime of coeval bimodal magmatism). Deformation occurred only twice by short-lived compressional deformation reflecting far-field effects of global orogenic events external to the proto-Congo Craton during Rodinia and Gondwana amalgamation.

Over the years, the term “Kibaran” became often mistakenly used in literature as synonym for “Mesoproterozoic” (1.6–1.0 Ga) and/or to denote Mesoproterozoic orogenic events in Africa. Other geologists restricted its use to the 1.0 Ga “global” collisional orogenic event at the edge of the Congo Craton, leading to Rodinia amalgamation, even if the (way of) participation of the African cratonic blocks in this process is still a matter of debate. Anyhow, “Kibaran” became synonymous to “Grenville” (= “Grenville-aged”) confusing African versus American geologists.

We propose that in future the use of the ambiguous term “Kibaran” – systematically in association with the term “event” – should be restricted to refer only to the c. 1375 Ma prominent tectono-magmatic event, which is unrelated to an orogenic event but includes intracratonic (i.e. intraplate) emplacement of abundant coeval bimodal magmatism under extensional regime (Tack et al., 2010).

Similarly, we redefined in this paper the Karagwe-Ankole Belt and the Kibara Belt – written as proper name and not as adjective – and propose to use these names in a purely descriptive and geographic sense without any geochronological or orogenic connotation.

In any case, the term “Kibaran” should be rejected for the ca. 1.0 Ga collisional processes at plate edges (including the related collisional granitic magmatism), at the origin of Rodinia amalgamation. Whether the term “Grenville-aged” is appropriate for (central) Africa by opposition to already previously used

African terms like (Southern) Irumide, Natal, Namaqua, is open for debate.

Acknowledgements

U–Pb measurements were conducted using the Perth SHRIMP ion microprobes at the John de Laeter Centre for Mass Spectrometry at Curtin University of Technology, in Perth, Australia by authors Cutten and De Waele.

The airborne magnetometry dataset was provided by the Faculty of Geo-Information Science and Earth Observation, University of Twente, Enschede, The Netherlands (formerly the International Institute for Aerospace Survey – ITC, Delft), and processed by author Barritt.

Appendix A. SHRIMP analytical procedures

Single-zircon U–Pb SHRIMP measurements were carried out by Cutten and De Waele. The complete analytical procedures are summarised in Tack et al. (2010). Individual zircons were separated from the samples, mounted and polished mid-section, together with the CZ3 zircon standard. Each mount was gold-coated and imaged to reveal size, colour, morphology, and internal zoning of the zircon grains, using a binocular microscope and a scanning electron microscope with a cathode-luminescence detector. The zircons were analysed on the sensitive high mass resolution ion microprobe (SHRIMP II) of the Perth Consortium. U–Pb SHRIMP methodologies followed Nelson (2001) and data reduction followed Clauqué-Long et al. (1995), using software by Ludwig (2001a,b) and Sircombe (2004). Corrections for common Pb were based on measured ^{204}Pb with the composition of common Pb chosen after Stacey and Kramers (1975) appropriate to the uncorrected $^{207}\text{Pb}/^{206}\text{Pb}$ age of each zircon. For detrital zircon, only data within 10% of concordia were used. Because all analysed zircons were older than 1.4 Ga, and because only concordant data are used, ^{204}Pb corrected $^{207}\text{Pb}/^{206}\text{Pb}$ ages are reported throughout. In case of the tuff, only clear, euhedral, uncracked and well-zoned non-complex zircons were analysed and yielded a concordant group from which a concordia age was calculated (Ludwig, 1998). Zircons from the quartzites were analysed indiscriminately to avoid biasing the result. All ages are reported at 95% confidence level.

References

- Andersen, L.S., Unrug, R., 1984. Geodynamic evolution of the Bangweulu block, northern Zambia. *Precambrian Research* 25, 187–212.
- Anonymous, 1990. Carte géologique du Burundi. 1:250,000, Ministère de l'Energie et des Mines, République du Burundi.
- Baudet, D., personal communication.
- Baudet, D., Tahon, A., Fernandez-Alonso, M., Tack, L., Theunissen, K., personal communication.
- Baudet, D., Hanon, M., Lemonne, E., Theunissen, K., 1988. Lithostratigraphie du domaine sédimentaire de la chaîne Kibarienne au Rwanda. *Annales de la Société Géologique Belge* 112, 225–246.
- Boven, A., Theunissen, K., Sklyarov, E., Klerkx, J., Melnikov, A., Mruma, A., Punzalan, L., 1999. Timing of exhumation of a high-pressure granulite terrane of the Palaeoproterozoic Ubende belt (west Tanzania). *Precambrian Research* 93, 119–137.
- Brinckmann, J., Lehmann, B., Hein, U., Höhndorf, A., Mussallam, K., Weiser, T., Timm, F., 2001. La géologie et la minéralisation primaire de l'or de la chaîne Kibarienne, nord-ouest du Burundi, Afrique orientale. *Geologische Jahrbuch Reihe, D* 101, 3–195.
- Buchwaldt, R., Toulkeridis, T., Todt, W., Ucakuwun, E.K., 2008. Crustal age domains in the Kibaran belt of SW-Uganda: combined zircon geochronology and Sm–Nd isotopic investigation. *Journal of African Earth Sciences* 51, 4–20.
- Cahen, L., 1952. Les Groupes de l'Urundi, du Kibali et de la Rusizi au Congo Oriental et Nord-Oriental. *Annales Société Géologique de Belgique LXXV (Mémoires)*, M3–M71.
- Cahen, L., Snelling, N.J., 1966. *The Geochronology of Equatorial Africa*. North-Holland Publishing Company, Amsterdam, 195 pp.

- Cahen, L., Lepersonne, J., 1967. The Precambrian of the Congo, Rwanda and Burundi. In: Kalervo Rankama (Ed.), *The Geologic Systems. The Precambrian*, 3. Interscience Publishers, USA, pp. 143–290.
- Cahen, L., Ledent, D., 1979. Précisions sur l'âge, la pétrogenèse et la position stratigraphique des "granites à étain" de l'Est de l'Afrique centrale. *Bulletin Société belge de Géologie* 88 (1), 33–49.
- Cahen, L., Ledent, D., Villeneuve, M., 1979. Existence d'une chaîne plissée protérozoïque supérieur au Kivu oriental (Zaire): données géochronologiques relatives au Supergroupe de l'Itombwe. *Bulletin Société belge de Géologie* 88 (1), 71–83.
- Cahen, L., Snelling, N.J., Delhal, J., Vail, J.R., Bonhomme, M., Ledent, D., 1984. *The Geochronology and Evolution of Africa*. Oxford University Press, Oxford, 512 pp.
- Chemale-Junior, F., Dussin, I., Alkmin, F., Martins, M.S., Queiroga, G., Armstrong, R., Santos, M., 2012. Unraveling a Proterozoic basin history through detrital zircon chronology: the case of the Espinhaço Supergroup, Minas Gerais, Brazil. *Gondwana Research* 22 (1), 200–206.
- Claoué-Long, J., Compston, W., Roberts, J., Fanning, C.M., 1995. Two Carboniferous ages: a comparison of SHRIMP zircon dating with conventional zircon ages and ⁴⁰Ar/³⁹Ar analysis. In: Berggren, W.A., Kent, D.V., Aubry, M.-P., Hardenbol, J. (Eds.), *Geochronology, Time Scales and Global Stratigraphic Correlation*. SEPM (Society of Sedimentary Petrology) Special Publication, pp. 3–21.
- Danderfer, A., De Waele, B., Pedreira, A.J., Nalini, H.A., 2009. New geochronological constraints on the geological evolution of Espinhaço basin within the Sao Francisco Craton – Brazil. *Precambrian Research* 170, 116–128.
- De Clercq, F., Muech, P., Dewaele, S., Boyce, A., 2008. The tungsten mineralisation at Nyakabingo and Gifurwe (Rwanda): preliminary results. *Geologica Belgica* 11 (4), 251–258.
- De Waele, B., Fitzsimons, I.C.W., 2007. The nature and timing of Palaeoproterozoic sedimentation at the southeastern margin of the Congo Craton; zircon U–Pb geochronology of plutonic, volcanic and clastic units in northern Zambia. *Precambrian Research* 159, 95–116.
- De Waele, B., Kampunzu, A.B., Mapani, B., Tembo, F., 2006. The Mesoproterozoic Irumide belt of Zambia. *Journal of African Earth Sciences* 46, 36–70.
- De Waele, B., Johnson, S.P., Pisarevski, S.A., 2008. Palaeoproterozoic to Neoproterozoic growth and evolution of the eastern Congo Craton: its role in the Rodinia puzzle. *Precambrian Research* 160, 127–141.
- De Waele, B., Fitzsimons, I.C.W., Wingate, M.T.D., Tembo, F., Mapani, B., Belousova, E.A., 2009. The geochronological framework of the Irumide Belt: a prolonged crustal history along the margin of the Bangweulu Craton. *American Journal of Science* 309, 132–187.
- Deblond, A., 1994. Géologie et pétrologie des massifs basiques et ultrabasiques de la ceinture Kabanga-Musongati au Burundi. *Annales du Musée Royal de l'Afrique Centrale, Tervuren (Belgique)*. *Sciences Géologiques* 99, 1–123.
- Deblond, A., Tack, L., 1999. Main characteristics and review of mineral resources of the Kabanga-Musongati mafic-ultramafic alignment in Burundi. *Journal of African Earth Sciences* 29, 313–328.
- Deblond, A., Punzalan, L.E., Boven, A., Tack, L., 2001. The Malagarazi Supergroup of SE Burundi and its correlative Bukoban Supergroup of NW Tanzania: Neo – and Mesoproterozoic chronostratigraphic constraints from Ar–Ar ages on mafic intrusive rocks. *Journal of African Earth Sciences* 32, 435–449.
- Delor, C., Theveniaut, H., Cage, M., Pato, D., Lafon, J.-M., Bialkowski, A., Roig, J.-Y., Neto, A., Cavongo, M., Sergeev, S., 2008. New insights into the Precambrian Geology of Angola: basis for an updated lithochronological framework at 1:2 000 000 scale. In: 22nd Colloquium of African Geology (CAG22), Hammamet, Tunisia, November 4th–6th 2008. Abstracts volume, pp. 52–53.
- Delvaux, D., Cibambula, E., Kadima, E., Kipata, L., Sebagenzi, S.N., Tack, L., Kabeya, S.M., 2011. Intracratonic evolution and tectonic stress in the Congo Basin. In: 23rd Colloquium of African Geology (CAG23), Johannesburg, South Africa, 8–14 January 2011. Abstracts volume, p. 113.
- Dewaele, S., Tack, L., Fernandez-Alonso, M., Boyce, A., Muech, P., 2007a. Cassiterite and columbite-tantalite mineralisation in pegmatites of the northern part of the Kibara orogen (Central Africa): the Gatumba area (Rwanda). In: 9th Biennial SGA Meeting, Mineral Exploration and Research: Digging Deeper, Dublin, Ireland, pp. 1489–1492.
- Dewaele, S., Tack, L., Fernandez-Alonso, M., Boyce, A., Muech, P., 2007b. Cassiterite mineralization in vein-type deposits of the Kibara orogen (Central Africa): Nyamiumba (Rutongo area, Rwanda). In: 9th Biennial SGA Meeting, Mineral Exploration and Research: Digging Deeper, Dublin, Ireland, pp. 1007–1010.
- Dewaele, S., Tack, L., Fernandez-Alonso, M., Boyce, A., Muech, P., Schneider, J., Cooper, G., Wheeler, K., 2008a. Geology and mineralization at the Gatumba area: Present state of knowledge. *Etudes Rwandaises* 16, 6–24.
- Dewaele, S., Tack, L., Fernandez-Alonso, M., 2008b. Cassiterite and columbite-tantalite (Coltan) mineralisation in the Proterozoic rocks of the northern part of the Kibara orogen (Central Africa): preliminary results'. *Bulletin Séances Académie Royale des Sciences d'Outre-Mer, Bruxelles* 54, 341–357.
- Dewaele, S., De Clercq, F., Muech, P., Schneider, J., Burgess, R., Boyce, A., Fernandez-Alonso, M., 2010. Geology of the cassiterite mineralisation in the Rutongo Area, Rwanda (Central Africa): current state of knowledge. *Geologica Belgica* 13, 91–112.
- Dewaele, S., Henjes-Kunst, F., Melcher, F., Sitnikova, M., Burgess, R., Gerdes, A., Fernandez-Alonso, M., De Clercq, F., Muech, P., Lehmann, B., 2011. Late Neoproterozoic overprinting of the cassiterite and columbite-tantalite bearing pegmatites of the Gatumba area, Rwanda (Central Africa). *Journal of African Earth Sciences* 61, 10–26.
- Fernandez-Alonso, M., 2007. Geological Map of the Mesoproterozoic Northeastern Kibara Belt. Royal Museum for Central Africa, Tervuren (Belgium): ISBN: 978-90-74752-12-1; catalogue of maps and digital data, at "<http://www.africamuseum.be>".
- Fernandez-Alonso, M., Lavreau, J., Klerkx, J., 1986. Geochemistry and geochronology of the Kibaran granites in Burundi, Central Africa: implications for the Kibaran Orogeny. *Chemical Geology* 57, 217–234.
- Fernandez-Alonso, M., Theunissen, K., 1998. Airborne geophysics and geochemistry provide new insights in the intracontinental evolution of the Mesoproterozoic Kibaran belt (Central Africa). *Geological Magazine* 135, 203–216.
- Fernandez-Alonso, M., De Waele, B., Tahon, A., Dewaele, S., Baudet, D., Cutten, H., Tack, L., 2009. The Northeastern Kibaran Belt (NKB): a 1250 Ma-long Proterozoic intracratonic history in Central Africa punctuated by two orogenic events at 1.0 and 0.55 Ga. Geological Society of London, Fermor Meeting, "Rodinia: Supercontinents, Superplumes and Scotland", Edinburgh, Scotland, 6–13 September 2009, Abstracts volume, p. 22.
- Fernandez-Alonso, M., Tack, L., Tahon, A., De Waele, B., 2011. The Proterozoic history of the Proto-Congo Craton of Central Africa. In: 23rd Colloquium of African Geology (CAG23), Johannesburg, South Africa, 8–14 January 2011. Abstracts volume, p. 142.
- Furon, R., 1958. *Géologie de l'Afrique*. Payot, Paris, p. 374.
- Geology and Mineral map of Tanzania (1:2,000,000), 2008. BRGM, Orléans, France.
- Gérards, J., Lepersonne, J., 1964. *Géologie du Nord-Est du Rwanda et stratigraphie du Burundi*. Musée royal Afrique centrale, Tervuren (Belgique), Département Géologie et Minéralogie, Rapport annuel, 1963, pp. 58–62.
- Gérards, J., Ledent, D., 1970. Grands traits de la géologie du Rwanda, différents types de roches granitiques et premières données sur l'âge de ces roches. *Annales Société Géologique Belgique* 93, 477–489.
- Gray, I.M., 1967. Quarter Degree Sheet 29 and 29W (Ngara). Mineral Resources Division of Tanzania, Dodoma.
- Johnson, S.P., De Waele, B., Liyungu, K.A., 2006. U–Pb sensitive high-resolution ion microprobe (SHRIMP) zircon geochronology of granitoid rocks in eastern Zambia: Terrane subdivision of the Mesoproterozoic Southern Irumide Belt. *Tectonics* 25, TC6004, <http://dx.doi.org/10.1029/2006TC001977>.
- Johnson, S.P., De Waele, B., Tembo, F., Katongo, C., Kenichero Tani, Qing Chang, Tsuyoshi Iizuka, Dunkley, D., 2007. Geochemistry, geochronology and isotopic evolution of the Chewore-Rufunsa Terrane, Southern Irumide Belt: a Mesoproterozoic Continental Margin Arc. *Journal of Petrology* 48 (7), 1141–1441.
- Jung, D., Meyer, F.M., 1990. Les méta-basites du Rwanda. IGCP No 255 Bulletin/Newsletter 3 (TU Braunschweig and RMCA, Tervuren), pp. 37–50.
- Kabengele, M., Lubala, R.T., Cabanis, B., 1991. Caractérisation pétrologiques et géochimique du magmatisme ubendien du secteur de Pepa-Lubumba, sur le plateau des Marungu (Nord-Est du Shaba, Zaire). Signification géodynamique dans l'évolution de la chaîne ubendienne. *Journal of African Earth Sciences* 13, 243–265.
- Kabete, J.M., Groves, D.I., McNaughton, N.J., Mruma, A.H., 2012. A new tectonic and temporal framework for the Tanzanian Shield: implications for gold metallogeny and undiscovered endowment. *Ore Geology Reviews*, 37, <http://dx.doi.org/10.1016/j.oregeorev.2012.02.009>.
- Kampunzu, A.B., Rumvegeri, B.T., Kapenda, D., Lubala, R.T., Caron, J.P.H., 1986. Les Kibarides d'Afrique centrale et orientale: une chaîne de collision. UNESCO, Geology for Economic Development, Newsletter/Bulletin 5, 125–137.
- Kampunzu, A.B., Makutu, M., Rocci, G., Kramers, J., Pineau, F., Louaradi, I., Tembo, F., 1997. Neoproterozoic Alkaline and Carbonatite Magmatism along the Western Rift in Central-Eastern Africa: break-up of Rodinia Supercontinent and reconstruction of Gondwana. *Gondwana Research* 1, 155–156.
- Kapenda, D., Kampunzu, A.B., Canabis, B., Namegabe, M., Tshimanga, K., 1998. Petrology and Geochemistry of Post-Kinematic Mafic Rocks from the Palaeoproterozoic Ubendian Belt, NE Katanga (DRC). *Geologische Rundschau* 87, 345–362.
- Klerkx, J., Liégeois, J.P., Lavreau, J., Theunissen, K., 1984. Granitoides kibariens précoces et tectonique tangentielle au Burundi: magmatisme bimodal lié à une distention crustale. In: Klerkx, J., Michot, J. (Eds.), *African Geology, A Volume in Honour of L. Cahen*. Royal Museum for Central Africa, Tervuren, pp. 29–46.
- Klerkx, J., Liégeois, J.-P., Lavreau, J., Claessens, W., 1987. Crustal evolution of the northern Kibaran Belt, eastern and central Africa. In: Kröner, A. (Ed.), *Proterozoic Lithospheric Evolution*, 17. American Geophysical Union and the Geological Society of America, pp. 217–233.
- Klerkx, J., Theunissen, K., Delvaux, D., 1998. Persistent fault controlled basin formation since the Proterozoic along the Western Branch of the East African Rift. *Journal of African Earth Sciences* 26, 347–361.
- Kokonyangi, et al., 2001. Geological Fieldwork in the Kibaran-Type Region, Mitwaba District, Congo (former Zaire), Central Africa. *Gondwana Research* 4, 255–259.
- Kokonyangi, J., Armstrong, R.A., Kampunzu, A.B., Yoshida, M., Okudaira, T., 2004. U–Pb zircon geochronology and petrology of granitoids from Mitwaba (Katanga, Congo): implications for the evolution of the Mesoproterozoic Kibaran belt. *Precambrian Research* 132, 79–106.
- Kokonyangi, J., Kampunzu, A.B., Poujol, M., Okudaira, T., Yoshida, M., Shabeer, K.P., 2005. Petrology and geochronology of Mesoproterozoic mafic–intermediate plutonic rocks from Mitwaba (D. R. Congo): implications for the evolution of the Kibaran belt in central Africa. *Geological Magazine* 142, 109–130.
- Kokonyangi, J., Kampunzu, A.B., Armstrong, R., Yoshida, M., Okudaira, T., Arima, M., Ngulube, D.A., 2006. The Mesoproterozoic Kibaride belt (Katanga, SE D.R. Congo). *Journal of African Earth Sciences* 46, 1–35.
- Kokonyangi, J., Kampunzu, A.B., Armstrong, R., Arima, M., Yoshida, M., Okudaira, T., 2007. U–Pb SHRIMP Dating of Detrital Zircons from the Nzilo Group (Kibaran Belt): implications for the source of sediments and Mesoproterozoic Evolution of Central Africa. *Journal of Geology* 115, 99–113.

- Lavreau, J., 1985. Le Groupe de la Rusizi (Rusizien du Zaïre, Rwanda et Burundi) à la lumière des connaissances actuelles. Musée royal Afrique centrale, Tervuren (Belgique), Dépt. Géologie Minéralogie, Rapport Annuel 1983–1984, pp. 111–119.
- Lenoir, J.L., Liégeois, J.-P., Theunissen, K., Klerkx, J., 1994. The Palaeoproterozoic Ubendian shear belt in Tanzania: geochronology and structure. *Journal of African Earth Sciences* 19, 169–184.
- Lepersonne, J., 1974. Carte géologique du Zaïre au 1/2 000 000 et notice explicative. République du Zaïre, Département des Mines, Direction de la Géologie, p. 67.
- Li, Z.X., Bogdanova, S.V., Collins, A.S., Davidson, A., De Waele, B., Ernst, R.E., Fitzsimons, I.C.W., Fuck, R.A., Gladkochub, D.P., Jacobs, J., Karlstrom, K.E., Lu, S., Natapov, L.M., Pease, V., Pisarevsky, S.A., Thrane, K., Vernikovsky, V., 2008. Assembly, configuration, and break-up history of Rodinia: a synthesis. *Precambrian Research* 160, 179–210.
- Liégeois, J.-P., personal communication.
- Ludwig, K.R., 1998. On the treatment of concordant uranium-lead ages. *Geochimica et Cosmochimica Acta* 62, 665–676.
- Ludwig, K.R., 2001a. *Isoplot/Ex rev. 2.49*. Berkeley Geochronology Centre, Berkeley, California, p. 54.
- Ludwig, K.R., 2001b. *Squid 1.02: A User's Manual*. Berkeley Geochronology Center, Berkeley, p. 19.
- Master, S., Bekker, A., Karhu, J.A., 2008. Palaeoproterozoic high delta13 carb marbles from the Ruwenzori Mountains, Uganda, and implications for the age of the Buganda-Toro Supergroup. In: 22nd Colloquium of African Geology, Hammamet, Tunisia, p. 90.
- Mbede, E.J., Kampunzu, A.B., Armstrong, R., 2004. Neoproterozoic Inheritance during Cainozoic rifting in the Western and Southwestern branches of the East African Rift System: evidence from Carbonate and Alkaline intrusions. The East African Rift System: Geodynamics, Resources and Environment, United Nations Conference Centre, Addis Ababa, Ethiopia, June 20–24, 2004, Extended Abstracts volume, p. 142.
- Muhongo, S., Tuisku, P., Mnali, S., Temu, E., Appel, P., Stendal, H., 2002. High-pressure granulite-facies metagabbros in the Ubendian Belt of SW Tanzania: preliminary petrography and *P-T* estimates. *Journal of African Earth Sciences* 34, 279–285.
- Navez, J., Karayenga, D., 1990. Geochemistry of sedimentary rocks from the Burundi Supergroup. IGCP 255, Bulletin/Newsletter, p. 109.
- Nelson, D.R., 2001. Compilation of SHRIMP U–Pb Zircon Geochronology Data, 2000. Geological Survey of Western Australia, Perth, Australia.
- Noce, C.M., Pedrosa-Soares, A.C., Silva, L.C., Armstrong, R., Pizana, D., 2007. Evolution of polycyclic basement complexes in the Araçuaí orogen, based on U–Pb SHRIMP data: implications for Brazil–Africa links in Palaeoproterozoic time. *Precambrian Research* 159, 60–78.
- Ntungicimpaye, A., 1981. Contribution à l'étude lithostratigraphique du Burundien inférieur dans la région de Mageyo (Burundi). Musée royal Afrique centrale, Tervuren (Belgique), Département Géologie et Minéralogie, Rapport annuel, 1980, pp. 161–171.
- Ntungicimpaye, A., 1983. Le magmatisme basique d'âge protérozoïque de la région de Mageyo (Burundi): données pétrographiques et géochimiques. Musée royal Afrique centrale, Tervuren (Belgique), Département Géologie et Minéralogie, Rapport annuel, 1981–1982, pp. 119–126.
- Ntungicimpaye, A., 1984. Contribution à l'étude du magmatisme basique dans le Kibarien de la partie occidentale du Burundi. Ph.D. Thesis (unpublished). University of Ghent (Belgium), 250 pp.
- Ntungicimpaye, A., Kampunzu, A.B., 1987. Caractérisation Géochimique des Metabasites Kibariennes (Proterozoïque Moyen) du Burundi. In: Matheis, G., Schandelmeier, H. (Eds.), 14th Colloquium of African Earth Sciences. Balkema, Berlin, pp. 37–40.
- Ntungicimpaye, A., Tack, L., 1992. Les métavolcanites intermédiaires à acides kibariennes du NW du Burundi. IGCP Project 255. Newsletter/Bulletin 4, 45–50.
- Nyakaa, J., Barritt, S.D., Ntulalalwo, V.B., Perez Almaguer, E.E., 1999. Transnational geophysical mapping of the Kibaran belt. In: UNESCO-IUGS, IGCP 418 and 419 Conference, 12–16 July 1999, Kitwe (Zambia), Abstracts volume, pp. 27–28.
- Pedreira, A.J., De Waele, B., 2005. The Palaeo/Mesoproterozoic sedimentary basins of the São-Francisco-Congo Craton: evolution and correlation. In: Gondwana-12: "Geological and Biological heritage of Gondwana", Mendoza, Argentina.
- Pedrosa-Soares, A.C., Alkmin, F.F., 2011. How many rifting events preceded the development of the Araçuaí-West Congo orogen? *Geonome* 19 (2), 244–251.
- Peeters, L., 1956. Contribution à la géologie des terrains anciens du Rwanda-Urundi et du Kivu. *Annales Musée royal du Congo belge, Tervuren (Belgique), Série in-8°. Sciences Géologiques* 16, 197.
- Pereira, E., Tassinari, C.C.G., Rodrigues, J.F., Van-Dunem, M.V., 2011. New data on the deposition of the volcano-sedimentary Chela Group and its Eburnean basement: implications for post-Eburnean crustal evolution of SW Angola. *Comunicações Geológicas* 98, 29–40.
- Pinna, P., Cocherie, A., Thiéblemont, D., Feybesse, J.-L., et Lagny, Ph., 1996. Geodynamic evolution and metallogenic controls in the East-African Craton (Tanzania, Kenya, Uganda). BRGM, Orléans, France. *Chronique Recherche Minière* 525, 33–43.
- Pohl, W., 1987. Metallogeny of the north-eastern Kibaran belt, central Africa. *Geological Journal* 22, 103–119.
- Pohl, W., 1994. Metallogeny of the northeastern Kibaran belt, central Africa – recent perspectives. *Ore Geology Reviews* 9, 105–130.
- Pohl, W. and Hadoto, D.P.M., 1990. Granite related Kibaran gold mineralisation at Mashong, Bushenyi District (SW-Uganda). IGCP No. 255 Bulletin/Newsletter 3 (TU Braunschweig and RMCA, Tervuren), pp. 61–67.
- Powell, C.M., Preiss, W.V., Gatehouse, C.G., Krapez, B., Li, Z.X., 1994. South Australian record of a Rodinian epicontinental basin and its mid-Neoproterozoic breakup (~700 Ma) to form the Paleo-Pacific Ocean. *Tectonophysics* 237, 113–140.
- Reddy, S.M., Collins, A.S., Mruma, A., 2003. Complex high-strain deformation in the Usagaran Orogen, Tanzania: structural setting of Palaeoproterozoic Eclogites. *Tectonophysics* 375, 101–123.
- Ring, U., Kröner, A., Toulkeredis, T., 1997. Palaeoproterozoic granulite-facies metamorphism and granitoid intrusions in the Ubendian-Usagaran Orogen of northern Malawi, east-central Africa. *Precambrian Research* 85, 27–51.
- Robert, M., 1931. Carte géologique du Katanga. *Nouv. Mém. Soc. Belge Géol. Paléont. Hydrol.* No. 5, 1 map scale 1/1:000:000. Explanatory Note, 14 pp.
- Rossetti, F., Cozzupoli, D., Phillips, D., 2007. Compression reworking of the East African Orogen in the Uluguru Mountains of eastern Tanzania at c. 550 Ma: implications for the final assembly of Gondwana. *Terra Nova* 20 (1), 59–67.
- Rumvegeri, B.T., 1991. Tectonic significance of Kibaran structures in Central and eastern Africa. *Journal of African Earth Sciences* 13, 267–276.
- Rumvegeri, B.T., Bingen, B., Derron, M.H., 2004. Tectonomagmatic evolution of the Kibaran Belt in Central Africa and its relationships with mineralizations; a review. *Africa Geoscience Review* 11 (1), 65–73.
- Schandelmeier, H., 1983. The geochronology of post-Ubendian granitoids and dolerites from the Mambwe area, northern province, Zambia. *Report Institute of Geological Sciences* 83, 40–46.
- Sircombe, K.N., 2004. Age display: an EXCEL workbook to evaluate and display univariate geochronological data using binned frequency histograms and probability density distributions. *Computers and Geoscience* 30, 21–31.
- Sklyarov, E.V., Gladkochub, D.P., Mruma, A., Theunissen, K., Melnikov, A.I., Klerkx, J., 1998. Paleoproterozoic eclogites and garnet pyroxenites of the Ubende Belt (Tanzania). *Schweizerische Mineralogische und Petrographische Mitteilungen* 78 (2), 257–271.
- Stacey, J.S., Kramers, J.D., 1975. Approximation of terrestrial lead isotopic evolution by a two-stage model. *Earth and Planetary Science Letters* 26, 207–221.
- Tack, L., 1995. The Neoproterozoic Malagarazi Supergroup of SE Burundi and its equivalent Bukoban System in NW Tanzania: a current review. In: Wendorff, M., Tack, L. (Eds.), Late Proterozoic belts in Central and Southwestern Africa; IGCP Project 302, Royal Museum for Central Africa, Tervuren (Belgium). *Geological Sciences* 101, 121–129.
- Tack, L., Ntungicimpaye, A., 1993. Le magmatisme basique dans le Kibarien de la région de Kayanza (Burundi). Musée royal Afrique centrale, Tervuren (Belgique), Département Géologie Minéralogie, Rapport annuel 1991–1992, pp. 179–181.
- Tack, L., De Paep, P., Deutsch, S., Liégeois, J.P., 1984. The alkaline plutonic complex of the Upper Ruvubu (Burundi): geology, age, isotopic geochemistry and implications for the regional geology of the Western Rift. In: Klerkx, J., Michot, J. (Eds.), African Geology, A Volume in Honour of L. Cahen. Musée Royal d'Afrique Centrale, Tervuren, Belgium, pp. 91–114.
- Tack, L., Sindayihebura, L., Cimpaye, D., 1992. The Nkoma (SE Burundi): an episodically reactivated lower Burundian siliciclastic sequence, locally overlain by a Malagarasian sedimentary breccia. IGCP No. 255 Newsletter/Bulletin 4 (TU Braunschweig and RMCA, Tervuren), pp. 9–22.
- Tack, L., Liégeois, J.P., Deblond, A., Duchesne, J.C., 1994. Kibaran A-type granitoids and mafic rocks generated by two mantle sources in a late orogenic setting (Burundi). *Precambrian Research* 68, 323–356.
- Tack, L., Deblond, A., De Paep, P., Duchesne, J.C., Liégeois, J.P., 1996. Proterozoic alignments of alkaline plutons revealing lithospheric discontinuities: evidence from Eastern Africa. In: Demaiffe, D. (Ed.), Petrology and Geochemistry of Magmatic Suites of Rocks in the Continental and Oceanic Crusts. A Volume Dedicated to Prof. J. Michot. Université Libre de Bruxelles and Royal Museum for Central Africa (Tervuren), Belgium, pp. 219–226.
- Tack, L., Baudet, D., Chartry, G., Deblond, A., Fernandez-Alonso, M., Lavreau, J., Liégeois, J.-P., Tahon, A., Theunissen, K., Trefois, Ph., Wingate, M., 2002a. The Northeastern Kibaran Belt (NKB) reconsidered: evidence for a c. 1370 Ma-old, repeatedly reactivated Kibara mobile belt, preceding the c. 1.0 Ga Rodinia Supercontinent assembly. In: 19th Colloquium of African Geology, El Jadida, Morocco, 19–23 March 2002, Special Abstracts volume, p. 173.
- Tack, L., Fernandez-Alonso, M., Tahon, M., Wingate, M.T.D., Barritt, S., 2002b. The "northeastern Kibaran belt" (KAB) and its mineralisations reconsidered: new constraints from a revised lithostratigraphy, a GIS-compilation of existing geological maps and a review of recently published as well as unpublished igneous emplacement ages in Burundi – 11th Quadrennial IAGOD Symposium and GEO-CONGRESS 2002, 22–26 July, Windhoek, Namibia, Synopsis of Extended Abstract (on CD-Rom). Conference Programme volume, p. 42.
- Tack, L., Fernandez-Alonso, M., De Waele, B., Tahon, A., Dewaele, S., Baudet, D., Cutten, H., 2006. The Northeastern Kibaran Belt (NKB): a long-lived Proterozoic intraplate history. In: 21st Colloquium African Geology (CAG21), 03–05.07.2006, Maputo, Mozambique, Abstract volume, pp. 149–151.
- Tack, L., Wingate, M., De Waele, B., Meert, J., Griffin, B., Belousova, E.A., Tahon, A., Fernandez-Alonso, M., Baudet, D., Cutten, H., Dewaele, S., 2008. The Proterozoic Kibaran Belt in Central Africa: intracratonic 1375 Ma emplacement of a LIP. In: 22nd Colloquium African Geology (CAG22), 04–06.11.2008, Hammamet, Tunisia, Abstract volume, p. 89.
- Tack, L., Wingate, M.T.D., De Waele, B., Meert, J., Belousova, E., Griffin, A., Tahon, A., Fernandez-Alonso, M., 2010. The 1375 Ma "Kibaran event" in Central Africa: prominent emplacement of bimodal magmatism under extensional regime. *Precambrian Research* 180, 63–84.
- Tack, L., Fernandez-Alonso, M., Tahon, A., De Waele, B., Baudet, D., Dewaele, S., 2011. The "Kibaran belt" of central Africa: What's in a name? In: 23rd Colloquium

- of African Geology (CAG23), Johannesburg, South Africa, 8–14 January 2011. Abstracts volume, p. 376.
- Tahon, A., 1990. The Kibaran structural pattern in Rwanda as the result of major lateral shear. In: Recent data in African Earth Sciences, Publication Occasionnelle CIFEG, Orléans, France, pp. 101–105.
- Theunissen, K., 1988. Kibaran thrust fold belt (D1-2) and shear belt (D2'). IGCP No 255 Bulletin/Newsletter 1 (TU Braunschweig and RMCA, Tervuren), pp. 55–64.
- Theunissen, K., 1989. On the Rusizian basement rise in the Kibara Belt of Northern Lake Tanganyika. Collision belt geometry or restraining bend emplaced in the late Kibaran strike-slip environment. IGCP No. 255 Bulletin/Newsletter 2 (TU Braunschweig and RMCA, Tervuren), pp. 85–92.
- Theunissen, K., Hanon, M., Fernandez-Alonso, M., 1991. Carte Géologique du Rwanda, 1:200.000. Service Géologique, Ministère de l'Industrie et de l'Artisanat, République Rwandaise.
- Theunissen, K., Klerkx, J., Melnikov, A., Mruma, A., 1996. Mechanisms of inheritance of rift faulting in the western branch of the East African Rift, Tanzania. *Tectonics* 15, 776–790.
- Torquato, J.R., Fogaça, A.C., 1981. Correlação entre o Supergrupo Espinhaço no Brasil, o Grupo Chela em Angola e as formações Nosib e Khoabendus da Namíbia. In: Anais do Simpósio sobre o Craton do São Francisco e suas Faixas Marginais, Salvador, pp. 87–98.
- Van Straaten, H.P., 1984. Contribution to the Geology of the Kibaran Belt in North-west Tanzania. UNESCO Geology for Development, Newsletter/Bulletin 3, 59–68.
- Villeneuve, M., 1980. Les formations précambriennes antérieures ou rattachées au Supergroupe de l'Itombwe au Kivu oriental et méridional (Zaïre). *Bulletin Société belge de Géologie* 89 (4), 301–308.
- Villeneuve, M., 1987. Géologie du synclinal de l'Itombwe (Zaïre oriental) et le problème de l'existence d'un sillon plissé pan-africain. *Journal of African Earth Sciences* 6, 869–880.
- Villeneuve, M., personal communication for Kampunzu, A.B., Armstrong, R., Chorowicz, J., Villeneuve, M.
- Villeneuve, M., Guyonnet-Benaize, C., 2006. Apports de l'imagerie spatiale à la résolution des structures géologiques en zone équatoriale: exemples du Précambrien au Kivu (Congo Oriental). *Photo-Interprétation* 4, 4, 3–22 et 59–67.
- Villeneuve, M., Chorowicz, J., 2004. Les sillons plissés du Burundien supérieur dans la chaîne Kibarienne d'Afrique centrale. *Comptes Rendus Geosciences* 336, 807–814.
- Walemba, K.M.A., 2001. Geology, geochemistry and tectono-metallogenic evolution of Neoproterozoic gold deposits in the Kadubu area, Kivu, Democratic Republic of Congo. Ph.D. Thesis (unpublished). University of the Witwatersrand, Johannesburg, South Africa, 491 pp.
- Walemba, K.M.A., Viljoen, M.J., Viljoen, R.P., 2004. Geological setting, genesis and evolution of the Twangiza gold deposit. Kivu, eastern D.R. Congo. In: *Geoscience Africa 2004 Conference, Abstracts Volume 2*, Johannesburg, 12–16 July 2004. University of the Witwatersrand, pp. 682–683.
- Walemba, K., Master, S., 2005. Neoproterozoic diamictites from the Itombwe Synclinorium, Kivu Province, Democratic Republic of Congo: Palaeoclimatic significance and regional correlations. *Journal of African Earth Sciences* 42, 200–210.
- Waleffe, A., 1966. Quelques précisions sur la position stratigraphique du "Nkoma" dans le Malagarasien du Burundi. Musée royal Afrique centrale, Tervuren (Belgique), Département Géologie Minéralogie, Rapport annuel 1965, pp. 82–84.